Assessment of the application possibilities for Ground Penetrating Radar as clogging measuring method in porous asphalt pavement roads

Boudewijn Mol

s1745913

Final Report BSc Thesis

Engineering Technologies

University of Twente

July 2021

1st supervisor	dr. S.R. Miller	1st external supervisor	dhr. W. Bouwmeester
2nd supervisor	MSc. Q. Shen	2nd external supervisor	dr. R.L. Koomans
2nd examiner	ir. D.W. Poppema		

ASPARi — Paving the way forward

de Wegen scanners

UNIVERSITY OF TWENTE.

Table of Contents

List of Figures

List of Definitions

Term	Definition
Clogging	Natural filling process of dirt and debris in pavements.
Porous asphalt	Asphalt pavement with a relatively high amount of voids.
ZOAB	Dutch type of porous asphalt which is widely used in practice in The Netherlands.
Becker test	Test to measure permeability of a pavement by using a constant falling head of water.
Drill core	A locally drilled core of a pavement that can be taken and examined elsewhere.
Dielectric constant (DC)/(eps)	A constant that describes the speed at which electromagnetic waves move through a particular material (GSSI Academy, 2020).
Ground Penetrating Radar (GPR)	A non-destructive method to visualise subsurface materials using radar pulses.
Electrical Resistivity Tomography (ERT)	A measuring technique that uses an electrical current through a rode and images the resistivity of the surrounding material.
Infrared Thermography (IRT)	A technique which uses the energy omitted by any object and images the temperature connected to this energy.

Abstract

Within the asphalt construction sector the phenomenon of clogging is observed in Dutch porous asphalt pavement roads (ZOAB). During clogging the pavement fills up the relatively high percentage of voids these roads are designed to have. Clogging is especially observed on emergency lanes since tire suction appears on regular traffic lanes. A clogged pavement performs less on water permeability. Current methods to measure clogging are mostly destructive (drill cores), time consuming and questionably reliable (Becker Test). Currently, asphalt pavements are periodically cleaned while the current state of a pavement with respect to clogging is hardly known. To strive for more efficient road maintenance, a competent and non-destructive measuring method is sought to estimate clogging. De Wegenscanners are a Dutch road scanning company that use GPR to perform analyses on pavements to achieve improved road management for their clients. This research first investigates the required elements for GPR as new clogging measuring method. It describes the necessary steps to turn GPR data into clogging estimations. Then an internal validating case study is performed on historic ZOAB data from De Wegenscanners. This case study clearly indicates the expected type of clogging especially on the emergency lane. Finally, multiple external validating methods are prescribed to further establish GPR as newly accepted clogging measuring method.

1.   Introduction

In this report, investigation is done into the possibilities of Ground Penetrating Radar (GPR) in porous asphalt concrete pavement roads (ZOAB) in collaboration with De Wegenscanners (*Translation from Dutch: The Roadscanners*) and ASPARI, a collective between the University of Twente and Dutch asphalt contractors to pursue asphalt research and innovation. This report will describe the proposed problem, research design, new method design and presentation and discussion of the validation of the performed case study.

1.1. Context

Humans have been transporting themselves since the beginning of time. According to a study from ECMT & OECD [1] (2002), the demand for transportation and infrastructure systems has always been growing, especially in the last century. They claim this is partly due to an increase in populations, car ownerships, urbanization, and industrial size. The way institutions in practice have tried to influence transportation and road travel demand used to be 'predict and provide'. This approach is switching towards a 'anticipate and manage' approach from the 21st century onwards according to OECD (2002). This manage aspect triggered a lot of research into road mixtures, performance/deterioration models, and pavement evaluation methods for instance. In Europe, approximately 90% of the roads nowadays are composed of some sort of asphalt mixture (NAPA & EAPA [2], 2011). This stresses the vital function of asphalt concrete (AC) in current infrastructure systems and society.

1.1.1. ZOAB pavements

Asphalt concrete (AC) can be divided into many kinds of asphalt types such as Coarse Graded Asphalt, Warm/ Cold Mix Asphalt and Porous Asphalt (PA) (PLM, 2019). This research will be focussed on the performance of a particular Porous Asphalt (PA) type known as ZOAB

---

[1] European Conference of Ministers of Transport & Organisation for Economic Co-operation and Development
[2] National/European Asphalt Pavement Association

(*Translation from Dutch: Very Open Asphalt Concrete*). In the Netherlands, 80% of current highways are constructed using this PA (Rijkswaterstaat, 2005).

Dutch ZOAB pavements are designed to contain a void percentage around 20% of the total volume. The main beneficial characteristics of ZOAB are sufficient noise reduction and permeability performance due to its relatively large amount of voids. The latter describes the pavements ability to discharge water efficiently due to its open structure (Hamzah et al., 2013). Efficient permeability enables the pavement to prevent hydroplaning and puddling, increase skid resistance, minimise splash- and spray water and therefore increase the vision and safety for its users (Madhu Lisha Pattanaik, Rajan Choudhary, 2017) (Fwa et al., 1999).

However, on many PA pavements a phenomenon called clogging is observed within three years of use (Scholz & Grabowiecki, 2007). Due to its open structure the pavement is subjectable to dirt and debris filling up its voids. This clogging of the pavement reduces its permeability, which is meant to be one of the main benefits of ZOAB (Yong et al., 2008). In the Netherlands clogging prominently appears on the emergency lanes of a highway rather than on the traffic lanes. This difference is caused by a suction and pumping effect of the many tires on the traffic lanes keeping themselves relatively clean. (Hamzah et al. 2013). As a result, maintenance is required to prevent advanced clogging on the emergency lanes.

1.1.2. Types of maintenance

Monitoring roads concerning clogging and possible interventions fall under the maintenance of the Dutch roads. Various types of maintenance can be distinguished namely, "*reactive, preventive, predictive, aggressive (TPM) maintenance*" (Swanson, 2001), and possibly more. They all vary on how pro-active the approach is and Swanson found that the more pro-active the maintenance approach is the better the performance of the subject. Defining these types of maintenance and connecting clogging estimation and ZOAB cleaning advice to these types of maintenances can contribute to improving efficient road management, something De Wegenscanners strive to achieve with their methods.

1.1.3. Maintenance in road pavement

Currently, the emergency lanes of ZOAB pavements are periodically cleaned using a PA cleaning machine. According to Burningham & Stankevich (2005), this type of maintenance is called *routine maintenance*. It prevents early deterioration of the pavement, is performed while the road is in use and happens after fixed periods. This routine maintenance can be improved by applying a more pro-active approach. To improve this type of maintenance and move towards predictive maintenance and efficient PA cleaning the amount of clogging of a given road strip at a certain moment in time needs to be monitored. Monitoring the clogging of pavements enables locally needed cleaning improving efficient road management. A new method to monitor clogging using GPR is what this research tries to design and validate.

2.   Research design

2.1. Problem definition

It is found that the amount of clogging is closely related to the permeability performance of the pavement, which can be measured. To measure the permeability of a PA pavement the vast majority of researches use the principle of a constant falling head in their tests (Y. Ma et al., 2020) (Moriyoshi et al., 2013) (Fwa et al., 1999). It allows a fixed amount of water to pass through the pavement and measures the time for the water to do so in order to calculate the permeability. In Dutch this pavement specific falling head test is best known as the Becker test described by CROW together with the Beheerraad Aanbesteden en Contracteren (*Translation from Dutch: Governing council Tenders and Contracting*) (2020). Leegwater et al. (2019) ignored the decrease in permeability due to clogging in their research. They stated that above a total void percentage of 18% all pores may be assumed to be suitable as water drain and pointed to the usual Becker test (Beheerraad Aanbesteden en Contracteren & CROW, 2020). However, X. Ma et al. (2020) found that at 18% of total voids approximately 80% of all pores function as water drain and that the previous assumption holds for pavements with a total void percentage above 25% (X. Ma et al., 2020) (Sansalone et al., 2008). Zhao et al. (2019) portray even lower percentages of interconnectivity. Therefore, this research aims to address clogging issues in Dutch roads and develop an easier and more scientific clogging measuring method on ZOAB pavements.

De Wegenscanners is a Dutch company focussed on visualizing complete roads quickly and thoroughly to strive for efficient pavement management. They use gamma-ray spectroscopy (GRS) and ground penetrating radar (GPR) to map road thickness and composition, locate sub-surface pipes and detect pavement deterioration while driving amongst daily traffic. Figure 1 shows one of their measuring vehicles. They look for application possibilities for their modern methods and innovative approaches to well-known problems (De Wegenscanners, 2020). Originating from the pavement construction sector De Wegenscanners get questions about the use of GPR in clogging estimates in ZOAB pavements. Clogging estimations on PA roads could potentially be done using GPR to

improve predictive maintenance. De Wegenscanners have gathered GPR data of ZOAB roads and aspire to investigate this new territory of data interpretation and visualization. When proven to be accurate this new method could function as a generally accepted alternative over the current methods and therefore create new business opportunities for De Wegenscanners. It could also kickstart more research into GPR in connection with clogging in which De Wegenscanners could have a leading role.

Figure 1 Mobile GPR and GRS vehicle from De Wegenscanners

So clogging is a well-known phenomenon in porous asphalt roads, which undermines the porous benefits it was designed to have. Many researches are dedicated to investigate clogging rates, design better measuring methods and improve porous asphalt cleaning methods. Currently clogging can be measured using the Becker test, where a constant head of water is passed through a pavement. This test is time consuming and its accuracy can be questioned scientifically. De Wegenscanners envision themselves as a pivotal player in measuring clogging with their Ground Penetrating Radar. Their GPR measurements could possibly indicate the amount of clogging to improve cleaning planning and therefore strive for efficient road management.

2.2. Objective

This research aims to show that GPR road data can be used to quantify the clogging of a specific ZOAB pavement at a certain moment in time. This can be used to determine where and when maintenance is needed.

2.3. Research questions

This research objective is formulated in the following main research question:

How and to which extent can the GPR data evaluation method quantify clogging in Dutch porous asphalt pavement roads (ZOAB) to enable predictive maintenance?

To support the search for an answer to the main research question several sub-questions will be answered in the meantime and are worth defining:

Phase 1: Theoretical analysis

- What non-destructive measurements methods are used in practice?
- What is the performance of the current measuring methods used?
- How can the dielectric constant be determined using GPR?
- What assumptions are needed to quantify clogging based on the dielectric constant?
- What are the limitations for GPR concerning clogging?

Phase 2: New GPR method design

- What are the requirements for suitable road data?
- What are the limitations of available road data?
- What preparation steps need to be done to the road data?
- What processing steps need to be performed?

Phase 3: Internal validation

- How significant are the observed differences in the dielectric constant?
- How reliable are the observed differences in the dielectric constant statistically?
- What is the relation between expected and observed differences?
- How do the different dielectric constant relate to the amount of clogging?

Phase 4: External validation procedure design

- How much do the conclusions about clogging improve predictive road maintenance?
- How useful is this GPR evaluation method for De Wegenscanners?

This research aims to answer the above questions and they can function as a checking mechanism on the progress of answering them.

3.   Theoretical Framework

The theoretical framework describes the scientific context this research is in. It explains the established theory that will be translated into practice in this work. Therefore this chapter also partly covers the methodology for *Phase 1: Theoretical analysis* (see the beginning of Chapter 5).

The permeability of pavements mainly has to do with the number of voids or pores it contains. In PA pavements the percentage of voids is a design requirement to make use of its conductive and auditive benefits when it is in use (VBW [3], 2016). Essentially, clogging of pavements can also be traced back to a decrease of this void percentage due to debris filling them up.

3.1.1. Non-destructive methods in asphalt pavements

From practice and other researches multiple types of non-destructive pavement measurement techniques are currently being used. (Ciampoli et al., 2019) The applications vary from void measuring and moisture presence to the detection of defects and structural details. Methods like Electrical Resistivity Tomography (ERT) (Maślakowski et al., 2014) (Cosenza et al., 2006) and Infrared Thermography (IRT) (Solla et al., 2014) (Abu Dabous et al., 2017) next to GPR. ERT is a measuring technique that uses an electrical current through a rode and images the resistivity of the surrounding material. ERT is highly effective and applicable to determine void percentages or moisture content. It could however be considered only semi-non-destructive since the rode has to be inserted into a small borehole. In practice it would result in rigorous planning of these boreholes, which is time and money intensive. Therefore it undermines important aspects, which this research strives for. IRT is a technique which uses the energy omitted by any object and images the temperature connected to this energy. (Abu Dabous et al., 2017) In doing this it can highlight spots of deterioration and moisture. It is perfectly suitable for mapping big slabs of pavement and highlighting main defect locations or moisture collections. However for this research the needed accuracy in void differences is too detailed to only use IRT. Then the IRT results would be merged with additional GPR measurements for example. It could however function as a supportive technique

---

[3] Vakgroep Bitumineuze Werken

to quickly scan larger road segments. Since it merely has a supportive addition to this research it is not considered any further and the focus is on GPR.

3.1.2. Method of GPR measuring in pavements

The void percentage of a pavement can be measured using Ground Penetrating Radar (GPR) since it has a relationship with the dielectric constant of the pavement.

An air-coupled antenna (antenna at De Wegenscanners is 2GHz) is mounted to a vehicle that is driving over a pavement in daily traffic. The antenna sends and receives signals. When a layer change appears (e.g. from the top layer to base layer) a part of the signal is reflected to the receiver while the rest of the signal travels deeper into the pavement until the next layer change (e.g. from base layer to subgrade layer). The receivers register the location (GPS), two-way travel time (indicating depth), and amplitude of the reflected signals. Figure 2 graphically shows the process of a GPR signal partially reflecting within a pavement for illustration.
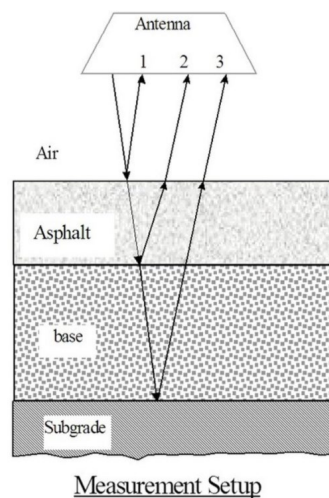
Figure 2 GPR signal traveling through a pavement (PAVEMENT STRUCTURE EVALUATION USING GPR, n.d.)

3.1.3. Dielectric constant in asphalt

The dielectric constant is a material characteristic that can be used to estimate the number of voids in asphalt pavement. Since air has a dielectric constant of 1, a relatively lower dielectric value in asphalt indicates a higher percentage of air and thus more voids on a dry road. The dielectric

constant is based on the reflection amplitude difference between measured radar reflection and the full reflection from a copper plate. A peak amplitude in the reflection indicates a layer change.

Figure 3 shows GPR reflection data with several peaks indicating different layers. This image can also be read rotated 90 degrees to the right where the signal travels across the depth of the pavement see Figure 4.
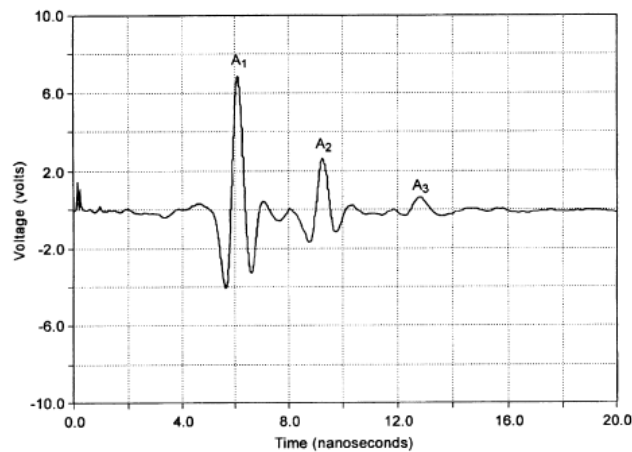
Figure 3 GPR reflections with peak amplitudes (Saarenketo & Scullion, 2000)
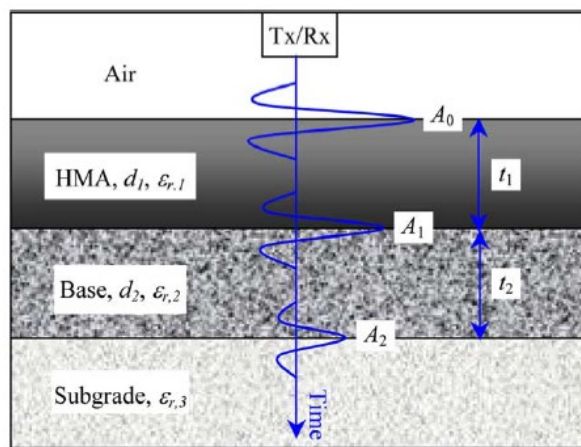
Figure 4 GPR reflection peaks along with the depth of the pavement (Al-Qadi & Lahouar, 2005)

The dielectric constant for the thin top layer

Saarenketo & Scullion (2000) defined a theoretical equation for the dielectric constant in the thin top layer of asphalt pavement, see Equation 1:

$$\varepsilon_a = \left[\frac{1 + \frac{A_1}{A_m}}{1 - \frac{A_1}{A_m}}\right]^2$$

(1)

Where, ε_a = the dielectric value of the thin top layer; A_1 = the amplitude of radar reflection from the asphalt; A_m = the amplitude of full reflection from a copper plate.

For the top layer, this formula and method are commonly used in practice, also at De Wegenscanners, to determine the thickness of the top layer or the void percentage. However, Figure 2 shows more peaks indicating more layer changes thus more layers. To estimate clogging of porous pavements the dielectric constant around the bottom of the porous top layer or in the second porous layer is of interest since clogging appears deeper in the asphalt package (*Translation from Dutch: asfalt pakket*). In other words, the dielectric constants can be determined on layer changes but they also address the behaviour of the dielectric constant around that layer change which is needed to estimate clogging.

The dielectric constant for deeper layers

To determine the dielectric constant on deeper layer changes a variable has to be defined for the decay of the signal based on the thickness of the above layers and the reflection coefficient of the above layers. More work into defining this expanded formula for two, three, and n-layers was done (Al-Qadi & Lahouar, 2005). This resulted in Equation 2 for n-layers:

$$\frac{A_n}{A_m} = \frac{\sqrt{\varepsilon_{r,n}} + \sqrt{\varepsilon_{r,n+1}}}{\sqrt{\varepsilon_{r,n}} - \sqrt{\varepsilon_{r,n+1}}} \left[\prod_{i=0}^{n-1}(1 - \gamma_i^2)\right] e^{-\eta_0 \sum_{i=0}^{n} \frac{\sigma_i d_i}{\sqrt{\varepsilon_{r,i}}}}$$

$$n = 0, 1, \ldots, N-1$$

(2)

Where ε_r = the dielectric constant for a layer; γ_i = the reflection coefficient given by Equation 3; η_0 = wave impedance of free space; σ_i = the conductivity of a layer; d_i = the thickness of a layer based on the two-way travel time of the signal (t_1) given by Equation 4. The conductivity σ_i used for this research is based on experiments from Opzoekingscentrum voor de Wegenbouw (2018).

$$\gamma_i = \frac{\sqrt{\varepsilon_{r,n}} - \sqrt{\varepsilon_{r,n+1}}}{\sqrt{\varepsilon_{r,n}} + \sqrt{\varepsilon_{r,n+1}}}$$

(3)

$$d_i = \frac{ct_i}{2\sqrt{\varepsilon_{r,i}}}$$

(4)

For this research, the equations are needed for two and three layers because two types of asphalt packages will be examined. Type 1 is a porous asphalt top layer that sits above a non-permeable base layer. Type 2 are two different kinds of porous asphalt layers on top of a base layer. The expansion of Equation 2 for two and three layers gives the following equations:

$$\varepsilon_{r,2} = \varepsilon_{r,1} \left(\frac{\left(1 - \left[\frac{A_0}{A_m}\right]^2\right) e^{-\eta_0 \frac{\sigma_1 t_1 c}{2\varepsilon_{r,1}}} + \left[\frac{A_1}{A_m}\right]}{\left(1 - \left[\frac{A_0}{A_m}\right]^2\right) e^{-\eta_0 \frac{\sigma_1 t_1 c}{2\varepsilon_{r,1}}} - \left[\frac{A_1}{A_m}\right]} \right)^2$$

(5)

$$\varepsilon_{r,3} = \varepsilon_{r,2} \left(\frac{\left(1 - \left[\frac{A_0}{A_m}\right]^2\right) e^{-\frac{\eta_0 c}{2}\left(\frac{\sigma_1 t_1}{\varepsilon_{r,1}} + \frac{\sigma_2 t_2}{\varepsilon_{r,2}}\right)} - \frac{\gamma_1 A_1}{A_m} + \left[\frac{A_2}{A_m}\right]}{\left(1 - \left[\frac{A_0}{A_m}\right]^2\right) e^{-\frac{\eta_0 c}{2}\left(\frac{\sigma_1 t_1}{\varepsilon_{r,1}} + \frac{\sigma_2 t_2}{\varepsilon_{r,2}}\right)} - \frac{\gamma_1 A_1}{A_m} - \left[\frac{A_2}{A_m}\right]} \right)^2$$

(6)

3.1.4. Connection between dielectric constant and void percentage

Laboratory experiments in Finland showed that the void percentage and the dielectric constant are in an exponential relationship with each other (Saarenketo & Scullion, 2000). However, Hoegh et al. (2015) noted that this relationship is based on empirical data fitting due to a dependency on the specific mix designs used. Several researches have been done into different in-situ asphalt mixtures and their effect on the asphalt density (Leng, 2011) (Leng et al., 2011). Next to this there are different mixing models to determine the bulk dielectric constant mentioned by Nelson (2005). Examples are the Complex Refractive Index Model (CRIM) (Brovelli & Cassiani, 2008), the Landau & Lifshitz, Looyenga model (LLL) (Dube, 1970), the Rayleigh equation (also known as the Maxwell

Garnett equation) (Ruppin, 2000), The Böttcher eqation (Fuller & Jr., 1953) (Yadav & Parshad, 1971) and the Bruggeman-Hanai equation (Shutko & Reutov, 1982). These different mixing models result in different relationships between the dielectric constant and the void percentage. The differences between the CRIM, LLL and Maxwell Garnett equation are compared by Pellinen et al. (2015), but here also a linear relationship was included. This linear relationship is based on the summation of the fractional dielectric constants, while these are weighed by their volumetric percentage, much like the CRIM and LLL models. The linear relationship is also shown by Jouyban et al. (2006). For this research this linear relationship is chosen. The limitations of this choice are later discussed in section 4.1.5. The linear equation is based on a formula for the determination of a cumulative dielectric constant, namely:

$$eps_{cum} = ((1 - \%_{air}) * eps_{asphalt}) + (\%_{air} * eps_{air})$$

(7)

The dielectric constant (*eps from the Greek letter epsilon*) for the dry asphalt materials used at De Wegenscanners is 5, which therefore is used here as well. This is supported by dielectric value ranges for dry materials used by Saarenketo (2006) and Fauchard et al. (2013). The dielectric constant for water and air are well known, namely 78.5 and 1 respectively (Wyseure, 2006). From Figure 5 and by substituting the known dielectric values in Equation 7 an equation for the relationship between the dielectric constant and void percentage can be derived, namely;

$$y = -4x + 5$$

(8)

This equation can be rewritten into a function x of y;

$$x = \frac{(5 - y)}{4}$$

(9)

Equation 9 can be used on measured dielectric constants to illustrate the behaviour of the void percentage along the segment for both the top and the bottom of the porous asphalt layer. This will later be discussed in section 6.2.6.

The chart shows a line plot with axis labels "DIELECTRIC CONSTANT" (y-axis, ranging 4.000 to 4.800) and "VOID PERCENTAGE (%)" (x-axis, ranging 0% to 25%), with the equation $y = -4x + 5$.
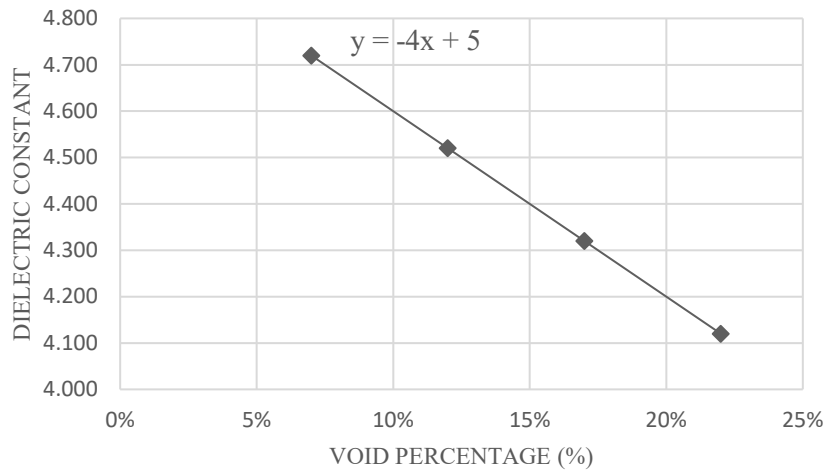
Figure 5 Relationship between the void percentage and the dielectric constant

3.1.5. Clogging estimates in practice

It is also worth mentioning that the dielectric measurements do not distinguish between pavement and clogging material. So the total void percentage may not be representative since the pavement was partially clogged at that moment. To tackle this, GPR measurements right after pavement cleaning are needed as a baseline and subsequently periodic measurements to determine the percentage of clogged voids. In an experimental setup with controlled clogging cycles, Garcia et al. (2019) reached potential clogging varying between 23% and 45%. Also Schaefer & Kevern (2011) and Tong (2011) simulated a clogging experiment to represent 20 years of service life and used twice the amount of clogging material than Garcia et al.. Their results indicate the importance of baseline and periodic measurements. More on this in Chapter 7.

For this research it is therefore needed that some assumptions are made, since the measurements are performed on a certain moment in time. To a certain extent some aspects need to be assumed about the conditions the measurements were taken in to ensure homogeneity of the data. The main assumptions concern, the boundaries of the chosen segments, homogeneity of the asphalt used and weather conditions during measurement. These aspects can be investigated and described but their effect on the measured data can not be taken into account. More information on these assumptions will be discussed later in section 6.2.

Also, there is a limitation to the use of GPR. The radar at De Wegenscanners is bound by its frequency of 2Ghz. If the frequency increases so does the resolution of the measured pavement, see Figure 6. This could increase the reliability of the data.

Depth increases

←

| 400MHz | — | 2GHz |

Resolution increases

→
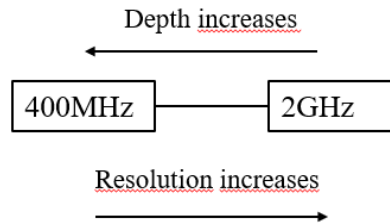
Figure 6 Trade-off based on radar frequency

Since for this research only the top layer of the pavement is investigated there is no bottom boundary for a depth that needs to be reached. In other words, the trade-off in frequency boundaries for this research is on the upper boundary at the resolution of 2GHz.

Next to this the research is limited by the chosen relationship between the dielectric constant and the void percentage, see section 4.1.4. The different mixing models vary from a linear relationship to a more exponential relationship. This difference can be caused by the different mixing model but also varies for different mixtures used from pavement to pavement. During the research also an exponential relationship has been analysed. This relationship was empirically determined by Saarenketo & Scullion (2000) and the equation is as follows:

$$y = 272.91 * e^{-1.3012 * x}$$

(10)

However, this linear relative to exponential relationship analysis based on the data from the case study, more on this in Chapter 6, showed no difference in the behaviour of the void percentage. Figure 7 and Figure 8 show this similar qualitative behaviour. There are differences in the values tough where the values of Figure 8, thus the linear relationship, indicates more clogging. Since this research aims to improve road management the indication of more clogging is in this case preferrable. Nevertheless, future research should try to examine the effect of different relationships

between the dielectric constant and the void percentage further and assess what is most applicable in practice.
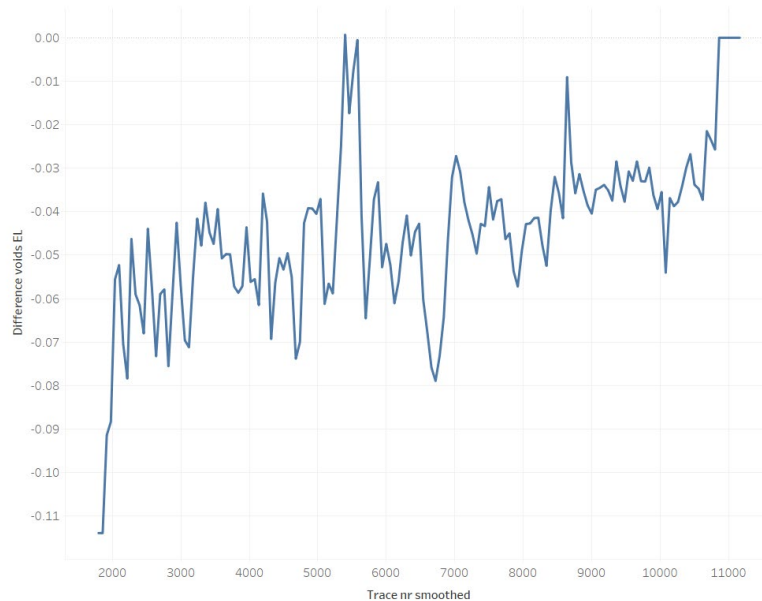
Figure 7 Void behaviour along a ZOAB pavement based on an exponential relationship
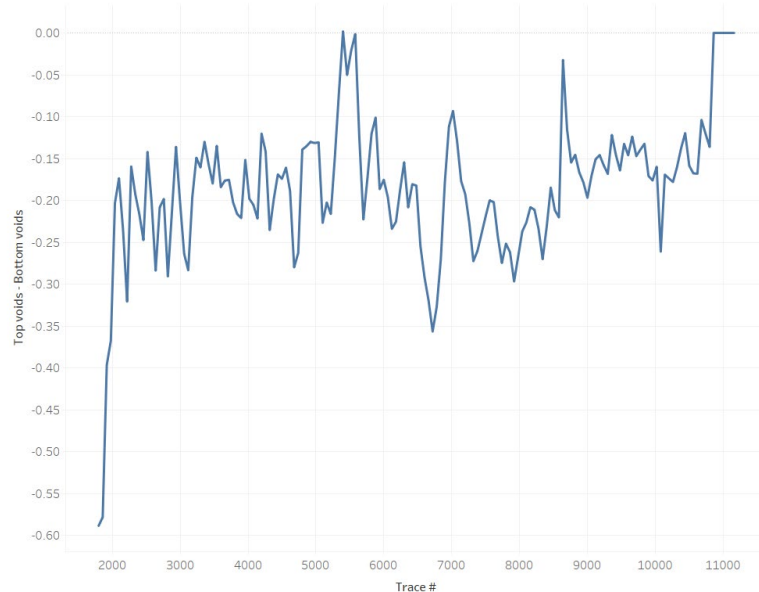
Figure 8 Void behaviour along a ZOAB pavement based on a linear relationship

So, in this research a linear relationship is chosen as main model to determine the void percentages. Picking a more complex mixing model to determine the void percentages could also introduce other assumptions and limitations. Therefore, the most straightforward linear relationship is chosen, also to simplify its application at De Wegenscanners.

4.   Methodology

The methodology describes the methods that will be used to perform this research. It indicates separate steps that need to be taken and the information flow between them which will lead to the result. The different phases underneath correspond to the phases described in section 3.3 .
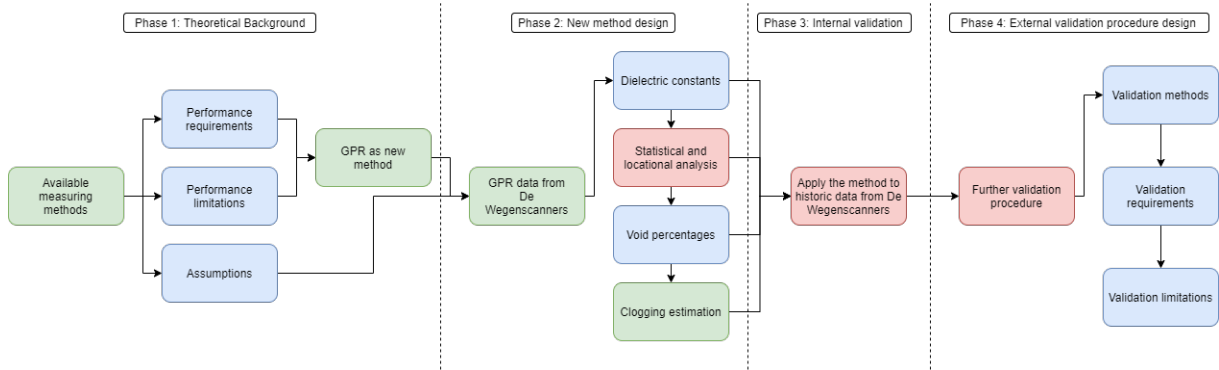
Figure 9 Design process flow diagram

Figure 7 Design process flow diagram shows the flow diagram for the design process. This diagram is based on the sub-questions from section 3.3 and divides the phases with the data (green), characterizing measurements (blue) and the analyses (red). It also shows the connection between the phases which will comprise the research. For each phase some textual explanation is useful to describe points of interest during the phase.

4.1. Phase 2: New GPR method design

De Wegenscanners have a large amount of GPR data from previous projects that are suitable for this research. During the data selection, specific segments of ZOAB pavements will be selected.

4.1.1. Data selection

This selection is mainly done based on the homogeneity of the asphalt mixture used throughout the different lanes to make data comparisons possible. The traffic lanes along one segment must consist of the same asphalt package and are measured during a relatively small time gap to eliminate weather influences between the lanes. This selection is done using data from drill core analysis which describes the asphalt package, a visual inspection by photo analysis and a check of open source top layer data in QGIS software. The photos are taken by the GPR vehicle during the

time of measuring. On these photos, different circumstances that influence the results could become apparent.

Next to the homogeneity of the asphalt, it is important to have distinct segments based on the defined Types of ZOAB pavement, see 6.1.12. This knowledge can also be extracted from the drill core data.

A final aspect that could come into play during the data selection is the stage of processing by De Wegenscanners. For the analysis performed by this research to succeed the different layers need to be auto-manually identified and marked in the radargrams. This ensures that the right amplitudes are exported and processed. Next to this, the data needs to have gone through several other general steps like basic noise reduction on the radargrams.

The data processing step seems intuitive and easy to make but defining it can help De Wegenscanners in the future. When a requirement list is made this can result in a set of boxes that need to be ticked in order for the data to be suitable for further analysis. However for it to be applicable in future projects it should be easy to check for De Wegenscanners and a concise but complete list of requirements and limitations can function as an easy and efficient method.

4.1.2. Data processing

After the ZOAB segments and the corresponding data are selected they need to be processed to eventually visualize dielectric constant differences over the lanes on multiple depths. This process begins with the exportation of the measured amplitude in the thin top layer. These measured amplitudes are displayed in the whiteness in the radargram but once exported are shown as a number in Volts. Figure 8 shows an example of such a radargram. From this picture the whiteness of the two marked lines is exported. This exportation happens from radargrams shown in the uniquely developed software from De Wegenscanners to Windows Excel, Figure 10 shows an example of such an Excel sheet. Here the dielectric constants have already been calculated, which will be explained underneath. Figure 11 shows the constants that are used to determine the dielectric constants.

filename	trace_nr	depth	amplitude	File	Trace_nr_2	zero_X_(ns	Amplitude_	Ametaal	eps_top	two-way travel time	eps_onder
200826AA_30001.	0	0.54	-128	200826AA_30001.	0	2.67	8906	31102.289	3.248921483	1.08E-09	3.191189845
200826AA_30001.	3	0.54	550	200826AA_30001.	3	2.67	9213	31102.289	3.392159341	1.08E-09	3.665632246
200826AA_30001.	6	0.54	251	200826AA_30001.	6	2.67	9513	31102.289	3.539178082	1.08E-09	3.66746718
200826AA_30001.	9	0.54	346	200826AA_30001.	9	2.67	8836	31102.289	3.217238279	1.08E-09	3.376780469
200826AA_30001.	12	0.54	327	200826AA_30001.	12	2.67	9030	31102.289	3.305925895	1.08E-09	3.461274343
200826AA_30001.	15	0.54	163	200826AA_30001.	15	2.67	9106	31102.289	3.341429877	1.08E-09	3.418916256

Figure 10 Example of an Excel data sheet with measurement variables and dielectric constants

no (impendance in free space)		c (speed of light in free space)			sigma (conductivity estimate)		
376.7303137		299792458			0.0001		
eps_top				eps_onder			
mean	std. Dev.	error		mean	std. Dev.	error	
3.815168135	0.235191547	0.004241991		3.789695476	0.387725586	0.006993145	

Figure 11 Example of an Excel data sheet with constants
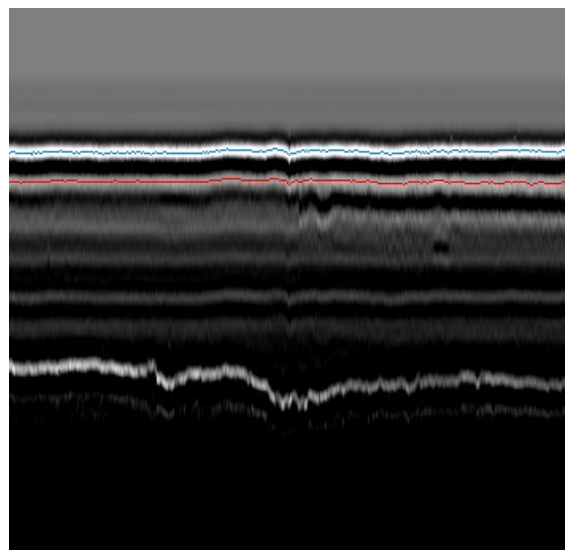
Figure 12 Example of a radargram with the top layer marked (blue = surface; red = bottom of top layer)

Within Excel, the full reflection of a copper plate is added corrected for the height of the antenna above the pavement. This correction is based on an empirical experiment performed by De Wegenscanners that defines a formula that needs to be accounted for on all measurements, see Figure 13. This shows the measured amplitude versus the height above the metal plate. After that, the dielectric values are determined for all measuring locations, with their corresponding coordinates. To evaluate this data statistically Tableau will used to visualize distributions and locational behaviour of the dielectric constants.
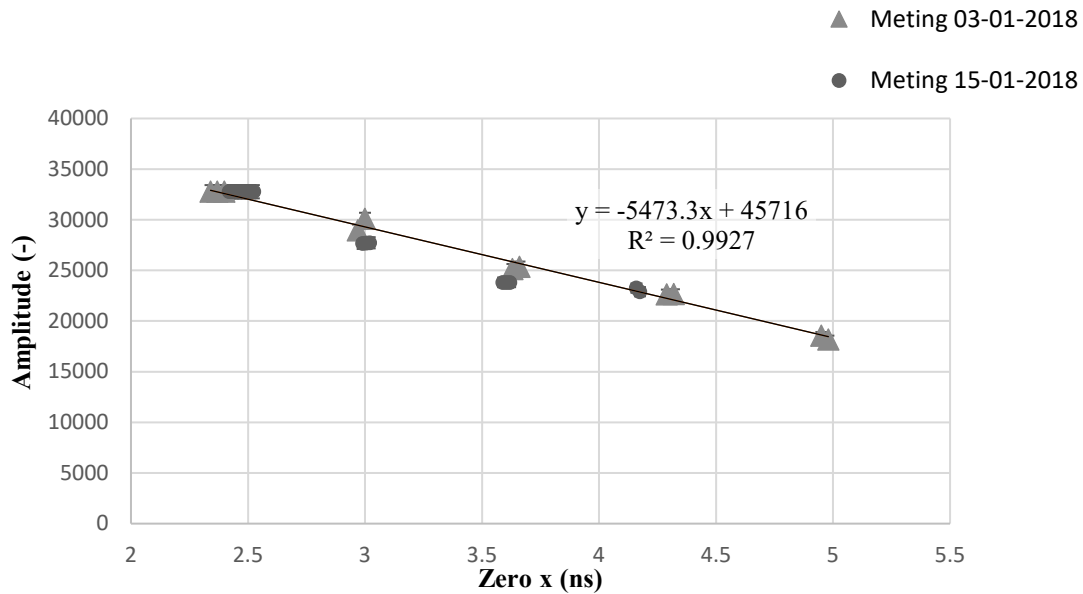
Figure 13 Empirical results for correction with the metal plate

The Excel data is also imported into the open-source software QGIS to visualize it. Here the dielectric values are displayed at their right location on a coloured scale, where red displays a high dielectric value, meaning relatively few influences of air ($\varepsilon_{air} = 1$) so relatively clogged, see Figure 10. This process is repeated for the different lanes and mapped on the specific ZOAB highway.
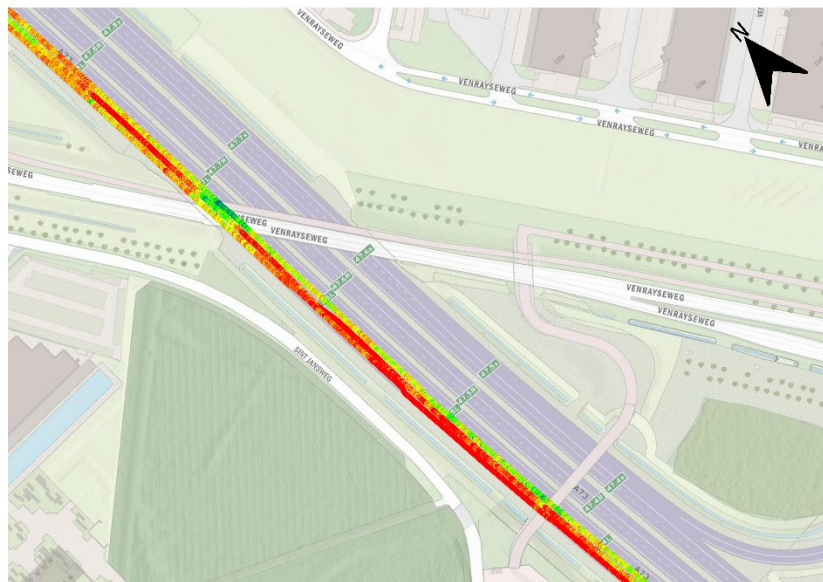
Figure 14 Example of scaled dielectric constants in QGIS

The techniques used here are chosen based on past experiences of De Wegenscanners, level of difficulty in use for the research and comprehensibility of the visualizations. At De

Wegenscanners the data exportations are done into Excel where mathematical formulas can be applied to the data to determine the dielectric constant. For the statistical analysis Tableau is chosen for its availability and the visually efficient mechanisms that contribute to the readability and thus comprehensibility of the research in the report. Alternatives of mathematical and statistical analysis could be Python coding. However this is not chosen since there is no experience with this at De Wegenscanners and for the student performing the research. This could affect the time efficiency greatly and also limit the usability and comprehensibility of the model for future applications. For the visualisation mainly QGIS is used, which connects the data values to their specific location and can show general behaviours of the data mapped on the road. Alternatives may vary to other Geo based software but QGIS was the easy choice since there is a lot of experience at De Wegenscanners with it.

So the newly designed method of GPR to estimate clogging proceeds as follows:

- **1. Export of the GPR data.** From the in-house software the reflection amplitudes at the surface and the bottom of the top layer are exported into an Excel sheet. This is done for all three lanes separately.
- **2. Mathematical conversion to the data.** All the amplitudes are converted in absolute dielectric constants for both the surface and the bottom of the top layer. This is done based on the equations from section 3.1.3. Also the data points are averaged per 20 data points to create more readable graphs later.
- **3. Locational check.** Then the data of all lanes are cross referenced in QGIS so that all lines in the Excel sheet correspond to the right location on the road. Also empty rows are deleted here. The results is an Excel sheet where one row shows the dielectric constants for that specific location.
- **4. Conversion from dielectric constant to void percentage.** Then for each lane and each data point the conversion is made to a void percentage. More on this in section 5.2.5.
- **5. Figures are constructed.** From the resulting data all the pictures are made in QIS and Tableau to visualize the behaviour of the measured dielectric constants and make them ready for interpretation.

4.2. Phase 3: Internal validation

In this phase part of the validation is performed on the new measuring method of GPR as described above. It entails an application of the design method to a case study of historic data De Wegenscanners gathered in 2020. It follows al the mentioned steps necessary to select, prepare and process the data. The results of this validating case study are presented in Chapter 26. By applying the method to a validating case study a first step is taken to scientifically strengthen the designed method, increase topical knowledge about the method an illustrate how further external validation

can be done. This can eventually lead to a general acceptance of GPR as clogging estimation method and it can be applied in practice throughout the sector.

4.3. Phase 4: External validation procedure design

The result of Phase 3 is a first insight in observed clogging at the case study and an insight in the procedure of the new designed method. After Phase 3 more elaborate and external validation is needed to strengthen the new method. There are several possible external validation methods that could ensure this development of the new method. Firstly, a comparison between the Becker test and GPR data on a current project can be performed. An alternative technique may be comparing measurements right before and right after vacuum cleaning of a certain porous asphalt road. Another external validation method could be taking periodic measurements an monitoring the clogging over a longer period of time. This could give an insight in the natural behaviour of clogging. Lastly, an experimental setup could be a solution where the natural phenomenon of clogging is simulated and measured. All these alternatives however require current or future road construction projects and communication and planning with the contractors. There are some contacts about possibilities but planning these generally takes a longer time than this research. So for this research a procedural design is done for these validation methods. This means this research will describe the possible methods more elaborately, highlight requirements for the validation methods and foresee limitations of the external validation methods.

The end result of this research is a newly designed measuring method to estimate clogging in porous asphalt pavements, internal validation of the methods by application to a case study and a descriptive roadmap for further external validation of the measuring method, that De Wegenscanners can perform, control and perfect themselves.

5.   Internal validation results

In this chapter the results will be described of a validating case study based on the proposed method of GPR to estimate clogging on a certain ZOAB pavement, see section 5.1. Also the research questions will be strived to answer that are described in section 2.3 under both *Phase 2: New GPR method design* and *Phase 3: Internal validation.*

This is an evaluation analysis on a 750m long segment of the A73 just north of the city of Venlo. On this segment GPR measurements are done on the 26th of August 2020 in southern direction. Based on these GPR measurements calculations are done for the dielectric constant. This evaluating analysis will describe observed behaviour based on the measurements and suggest possible causes for this behaviour.

5.1. Data description and preparation

This section describes the requirements and limitations of the road data used and with that indicates important requirements about homogeneity and situational conditions for any dataset in this type of analysis.

5.1.1. Location and layout

The A73 is a highway in the south of the Netherlands, see Figure 15. It connects the province of Limburg from the north to the south. The segment for this analysis sits between markers 47,2 and 48,0 on the left side, see Figure 15 (blue line). The A73 segment here consists of three traffic lanes and an emergency lane, see Figure 16. The right traffic lane functions as a insertion and exit lane on this segment.

Figure 15 Highway 73 in the southeast of The Netherlands with segment
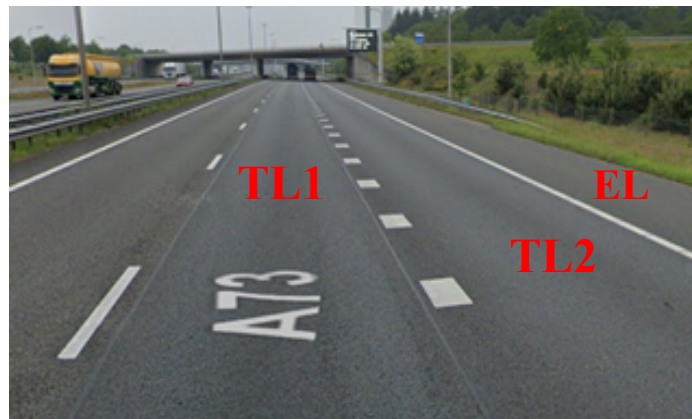
Figure 16 Layout of the A73 at observed segment with lane markings

5.1.1. ZOAB package

The ZOAB package (*describes the types and thicknesses of layers that are used*) is deducted from performed drill cores. The locations of these drill cores is visible shown by the white square markings in Figure 17. From the three clusters of drill cores the most eastern in not taken into account, since these fell outside the evaluated lanes.
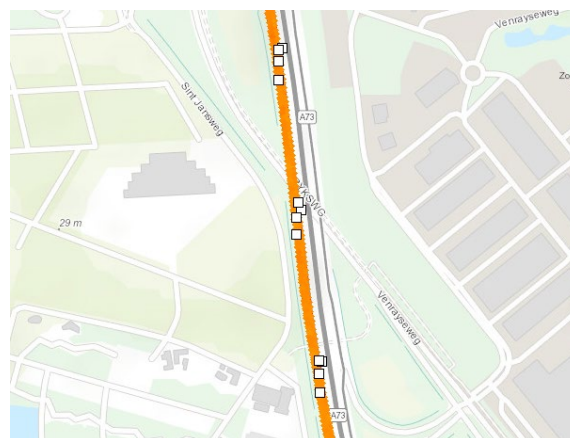
Figure 17 Segment with locations of the drill cores

Table 1 shows the results from the drill core analysis. From this analysis it can be seen that on this segment one surface layer of porous asphalt is used (ZOAB16). Underneath that lies a base layer. The drill core number corresponds to the lane markings from Figure 17, where cores 4-1, 4-4 and 4-7 correspond to TL1 (Traffic Lane 1), cores 4-2, 4-5 and 4-8 to TL2 (Traffic Lane 2) and cores 4-3, 4-6 and 4-9 to EL (Emergency Lane).

Table 1 Top and base layer types and depths from drill core analysis

| Drill nr.	Hardening	Type of top layer	Depth (mm)	Type of base layer	Depth (mm)
4-1	Asphalt	ZOAB16	55	STAB16	45
4-2	Asphalt	ZOAB16	53	STAB16	44
4-3	Asphalt	ZOAB16	55	STAB16	41
4-4	Asphalt	ZOAB16	46	STAB16	47
4-5	Asphalt	ZOAB16	53	STAB16	45
4-6	Asphalt	ZOAB16	53	STAB16	50
4-7	Asphalt	ZOAB16	44	STAB16	50
4-8	Asphalt	ZOAB16	50	STAB16	53
4-9	Asphalt	ZOAB16	60	STAB16	48

5.1.2. Measurements taken

The measurements that are taken are GPR data and gamma-spectro data for each lane. For every lane the position of the antenna was on the right (in driving direction). So all the data is gathered at the right side of the lane. For this analysis only the GPR data are of interest in combination with the drill cores and open source weather data. The GPR data will offer information of reflection amplitudes at different layers within the asphalt package. On this segment the data consist of approximately 3000 data points along the segment, which means;

$$3000 \ data \ points / \ 750 \ meter \ = \ 4 \ datapoints/meter \ .$$

So on all the lanes there is data measured approximately every 25 cm. To create more readable graphs all dielectric values and void percentages are averaged for every 20 data points. This means the pavement is assumed to be homogeneous within 5 meters along the segment. More analysis, like semi-variogram analysis, could be done to further establish the best amount of data points to make this assumption.

5.1.3. Weather conditions

The weather conditions during the time of measuring are important since wet conditions would give strikingly different results than dry asphalt conditions, more in section 6.2.5. Since the dielectric constant of water, ε_{water}= 81 and of air, ε_{air}= 1.

From (KNMI, 2020) the accumulated weather data is gathered for the week leading up to the measurements and the actual rain on the day of measuring (19-08-2020 until 26-08-2020). This results in no accumulated rain leading up to the measurements and 0,5 mm of rain on the 26th. This could affect the results from this analysis marginally. However it is assumed that the measurements between the lanes are performed in a relatively small time span, so their conditions are assumed to be similar.

5.1.4. Other particularities

There are two structures on this segment that could have an effect on the results. First an overhead road that is relatively wide and crosses the segment from the southeast to the northwest. Next to that a little further south another overhead road but which is narrower and crosses from east to west. The two structures can be seen in Figure 18.

Figure 18 Two structures on the segment. Left: larger overhead road. Right: smaller overhead road

5.1.5. Preparation steps needed

The measured GPR data needs to be prepared before the right amplitude can be exported and evaluated. So the raw GPR data needs to be altered before radargrams look the way they do in the software. Benedetto et al. (2017) extensively describes this sorting and filtering of data to eliminate unnecessary errors and therefore increase the accuracy of the data interpretation. In practice at De Wegenscanners several of the described steps are made. Based on a expert interview I had with

the head of all data analysis at De Wegenscanners the main preparation steps are defined. The necessary steps mainly focus on eliminating noise from the radargrams and identifying the surface line of the pavement and the bottom of the top layer so that the measured amplitudes can be exported on the right locations.

5.2. Data analysis

In this section the steps performed to the data will be named as well as the description of the results that followed from the method applied.

5.2.1. What differences do we see in the data?

In the data differences in the dielectric constant are expected. This can be differences within one lane or differences between the lanes. However at first it is desired to know the magnitude of the measured differences. This can be done by analysing the averages of the dielectric constants and the histograms. Table 2 displays the averages of the dielectric constants for each of the lanes at the two depths. The abbreviations for the lanes correspond to the labels in Figure 16.

Overall the average values are in the realm of the dielectric constant for porous asphalt roads. It can be seen that the averages increase from the middle of the road to the edge (from TL1 to EL). It can also be seen that these differences are larger on the bottom of the asphalt package than on the top.

Table 2 Averages of the dielectric constants

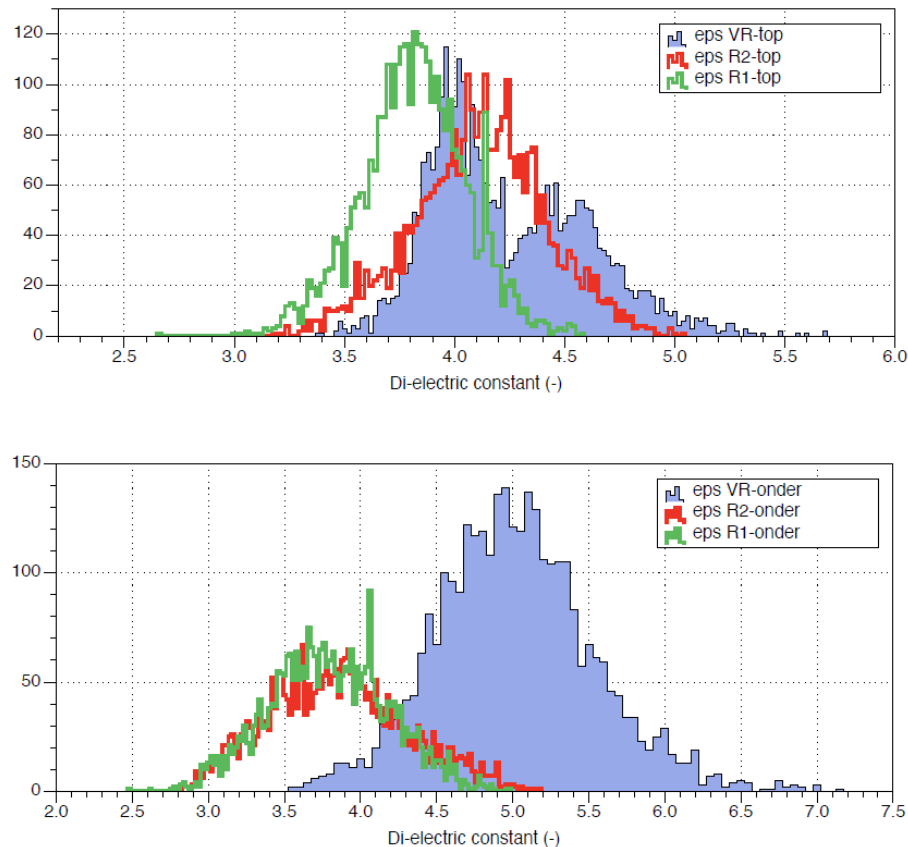|	TL1	TL2	EL
	Mean	**Mean**	**Mean**
Top	3.82	4.11	4.24
Bottom	3.79	3.84	5.02

Figure 19 Histograms of all dielectric values on top (top) and the bottom (bottom)

Figure 19 shows the histograms for all the measured dielectric constants. This proves the differences in the averages from Table 2. It also shows that the top of the EL the values behave differently than for the other measurements. It clearly shows two peaks instead of the other measurements which who one normal distributed peak.

5.2.2. What do the observed differences indicate?

To further comprehend the observed differences some further analysis can be functional. Firstly, the comparison between the observed differences and the standard deviations or deviation per point can be interesting. This can give some indication that the observed differences are caused by other factors than the spread in the data. Secondly it can be useful to have an indication what amounts of voids need to be filled up in order to achieve the observed differences.

5.2.3. Observed differences vs. data spread

To compare the observed differences with the deviation per point a semi-variogram can be used. In this analysis a certain amount of data points will be assumed homogeneous and from those

the standard deviation is determined. The average of these standard deviations can be compared to the observed differences in the data. The amount of data points that are assumed to be homogenous can vary to make several comparisons.

For 20 data points (5 meter of road) this leads to the standard deviations in Table 3. The 20 points will for now be used however further semi-variogram analysis can indicate that this is a applicable assumption. It shows that the observed differences from Table 2 are larger than the standard deviations per 20 points. This indicates that the observed differences are caused by other effects than the spread in the data. Therefore it is worthwhile to analyse what might cause these differences. This also corresponds to the averaging of every 20 points in the locational analysis.

Table 3 Average standard deviations per 20 data points

	TL1	TL2	EL
	Avg. st. dev.	Avg. st. dev.	Avg. st. dev.
Top	0.138	0.144	0.152
Bottom	0.180	0.192	0.255

5.2.4. Observed differences vs. Clogging estimations

The observed differences can be compared to rough estimations of the amount of clogging Lets say the initial porous asphalt road here was designed to contain 20% air voids and 80% dry asphalt materials. Table 4 shows an estimation for the effect of clogging on the dielectric constant. In this case two scenario's are observed where on one side the air voids clog with dirt and other asphalt like debris while on the other side the voids clog with water.

The average dielectric constants measured at the road segment in this analysis correspond to the clogging estimation where the voids fill up with dirt. The values with water filled voids increase much larger than observed here. This could indicate that less voids directly influence the dielectric constant and that this clogging phenomena could very well be applicable to this segment of the A73.

Table 4 Dielectric constant estimations

Air fills up with dirt	Ingredient	Percentage (%)	Eps.		Ingredient	Percentage (%)	Eps.		Ingredient	Percentage (%)	Eps.		Ingredient	Percentage (%)	Eps.
	Asphalt	78%	5		Asphalt	78%	5		Asphalt	78%	5		Asphalt	78%	5
	Air	22%	1		Air	17%	1		Air	12%	1		Air	7%	1
	Water	0%	78.5		Water	0%	78.5		Water	0%	78.5		Water	0%	78.5
	Dirt	0%	5		Dirt	5%	5		Dirt	10%	5		Dirt	15%	5
		100%				100%				100%				100%	
		Eps. abs.	4.120			Eps. abs.	4.320			Eps. abs.	4.520			Eps. abs.	4.720

Air fills up with water	Ingredient	Percentage (%)	Eps.		Ingredient	Percentage (%)	Eps.		Ingredient	Percentage (%)	Eps.		Ingredient	Percentage (%)	Eps.
	Asphalt	78%	5		Asphalt	78%	5		Asphalt	78%	5		Asphalt	78%	5
	Air	22%	1		Air	17%	1		Air	12%	1		Air	7%	1
	Water	0%	78.5		Water	5%	78.5		Water	10%	78.5		Water	15%	78.5
	Dirt	0%	5		Dirt	0%	5		Dirt	0%	5		Dirt	0%	5
		100%				100%				100%				100%	
		Eps. abs.	4.120			Eps. abs.	7.995			Eps. abs.	11.870			Eps. abs.	15.745

5.2.5. Locational analysis

For the locational analysis the dielectric constants will be observed along the road segment per lane at two depths, on the top of the porous asphalt layer (so the top of the pavement) and at the bottom of the porous asphalt layer. At first merely the observed behaviour will be described, which later will be translated to a void percentage for the two depths and then a void difference, see section 6.2.6. The location is based on the Trace number. This trace number is generated during measurements with the radar and a trace number is connected to each data point. Figure 16 displays the locations of the trace numbers. These locations can be compared to later figures with respect to the dielectric constants on certain locations.
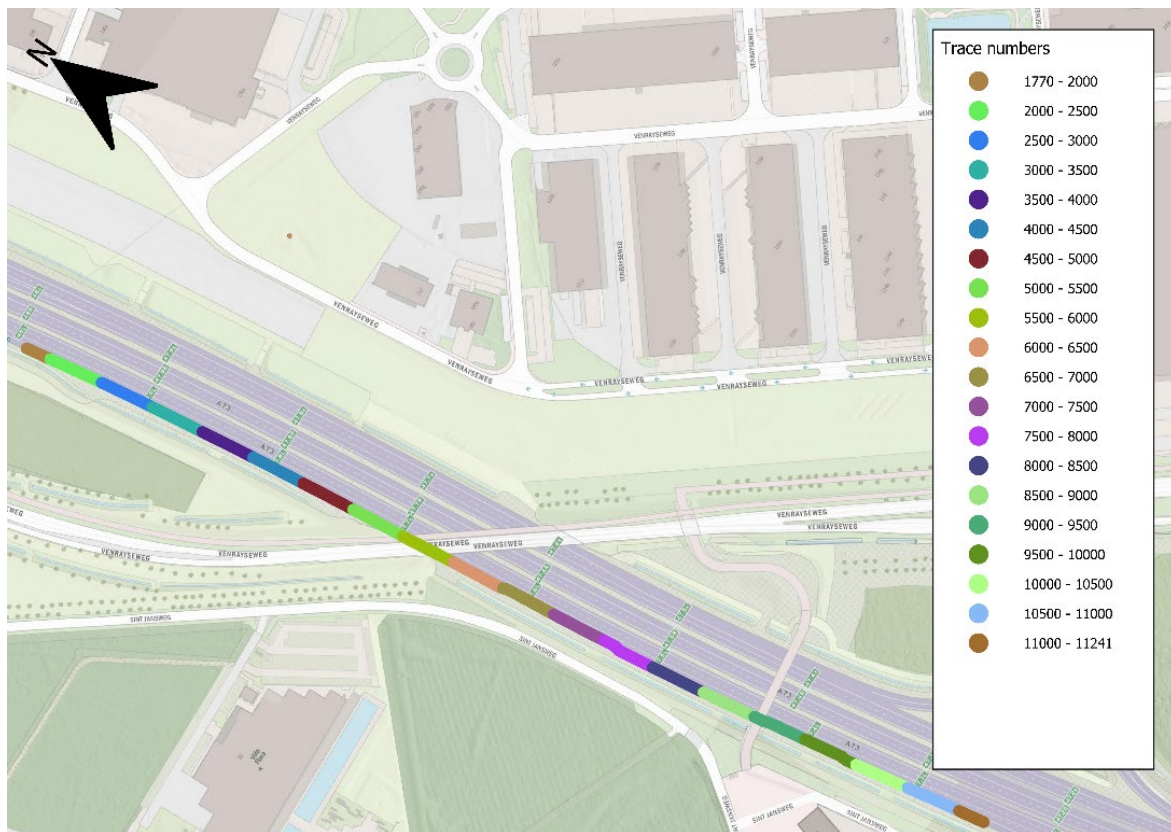

Figure 20 Trace numbers mapped on the A73 segment

Traffic Lane 1 (TL1)

Figure 21 shows the dielectric constant for TL1. It can be observed that the dielectric constant in the bottom is higher than on top in the first half and this is the other way around in the second half. In Figure 21 three different stages can be observed, highlighted by the red circles with a corresponding number. In stage 1, the dielectric constant (DC) of the bottom sits above the DC on top. In stage 2, this is the other way around and both DC's are lower relative to stage 1. In stage 3 it can be observed that the DC's are comparable to stage 2 but with smaller differences and that the DC's start to increase to the level comparable to stage 1. Furthermore, two clear drops of the DC can be observed at trace number 5700 and trace number 9200, coinciding with the locations of the overhanging structures.
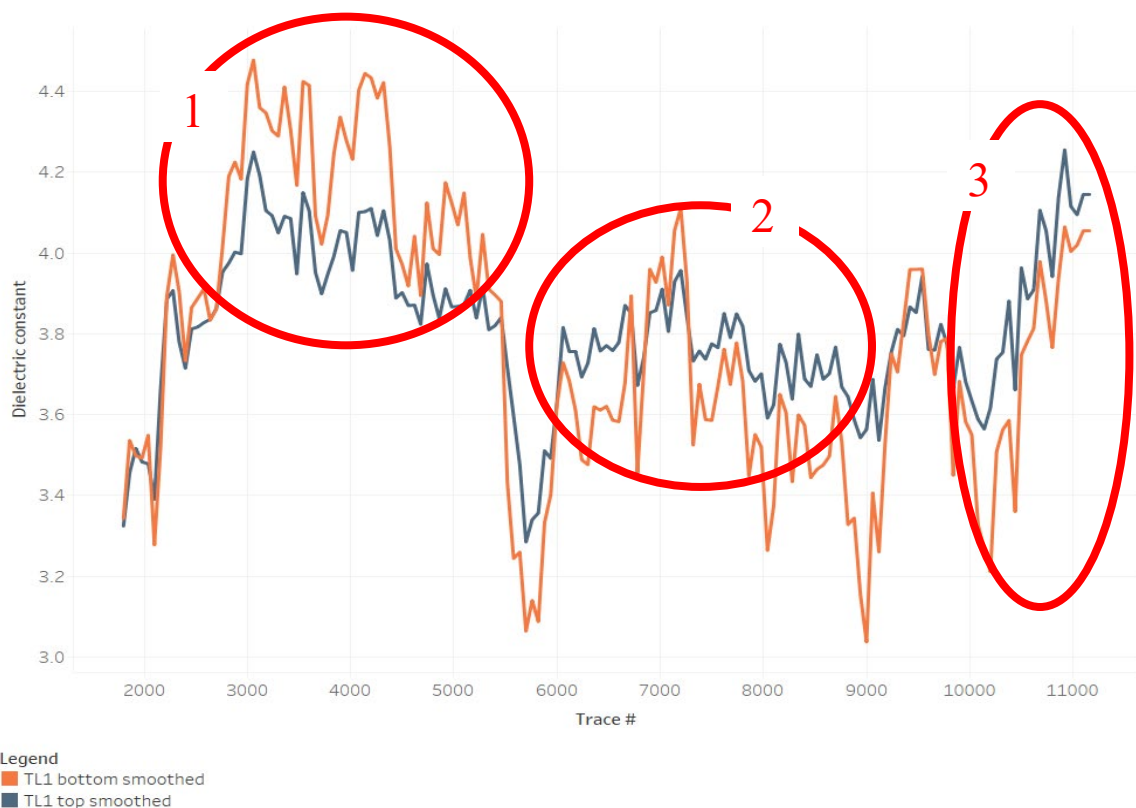

Figure 21 Smoothed dielectric constants along the segment at TL1

Traffic Lane 2 (TL2)

Figure 22 shows the dielectric constants on this road segment for TL2. It can clearly be seen that the bottom DC is lower than the top with some exceptions where they behave similar. Next to this again the dip at around trace number 5700 and 9200 can be observed. On TL2 two main stages can be seen as shown in Figure 18. In both stages the DC of the bottom is lower than the DC on top. However, in stage 1 the difference is relatively larger than in stage 2.

Figure 22 Smoothed dielectric constants along the segment at TL2

Emergency Lane (EL)

Figure 23 shows the dielectric constant on the EL. It can clearly be seen that the dielectric constant of the bottom is higher than of the top everywhere. Again dips can be seen at the same trace numbers as on TL1 and TL2.
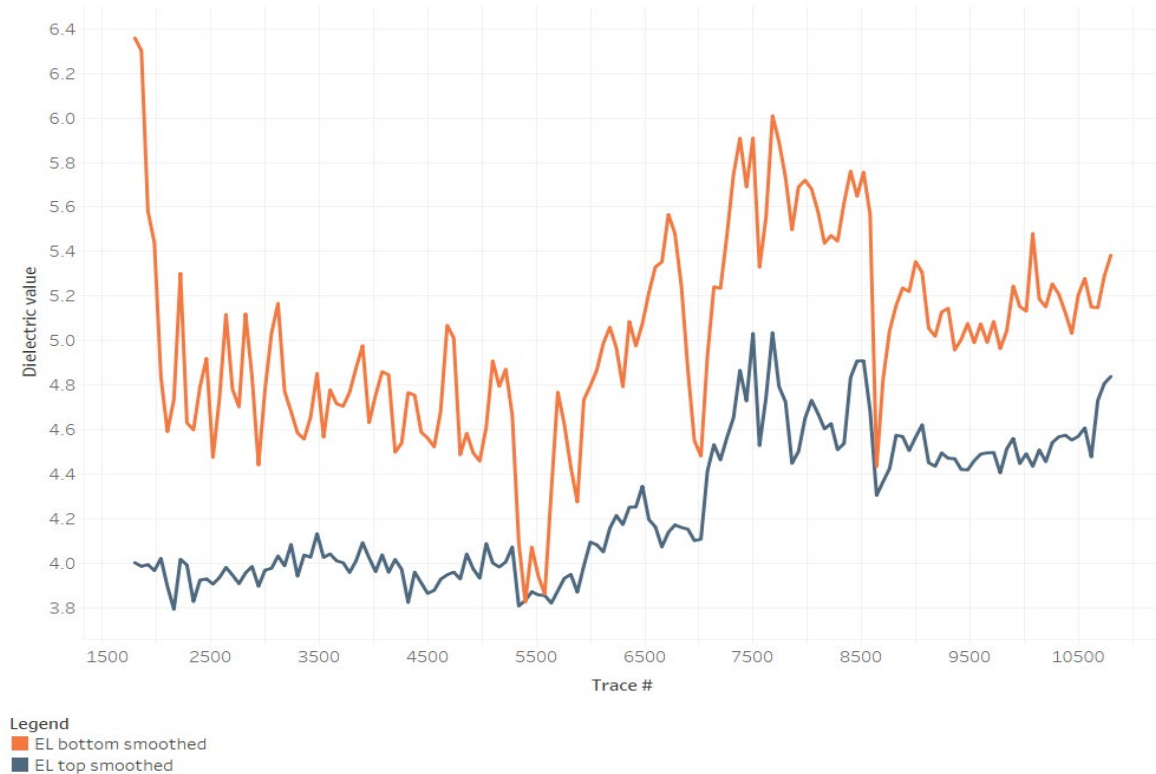
Figure 23 Smoothed dielectric constants along the segment at EL

5.2.6. Void analysis

The measured dielectric constants in combination with the formula from section 4.1.4 can be converted into a void percentage. This results in new graphs that be plotted to visualize the void percentage on the top and the bottom for all lanes. This is portrayed in Figure 26, Figure 28 and Figure 30. When subtracting the top voids from the bottom voids an estimation is given for the change of voids within the top layer. This could potentially show the clogging that happens in this road segment. This is shown in Figure 27, Figure 29 and Figure 31. In these three graphs a positive difference indicates a void increase, while a negative difference shows a void decrease.

Within these three graphs there are essentially three different scenario's possible: 1) The amount of voids does not chance throughout the top layer, 2) The amount of voids decreases throughout the top layer and 3) The amount of voids increases throughout the top layer, see Figure 20. A decrease and increase in the amount of voids on its turn indicates more or less clogging, respectively.
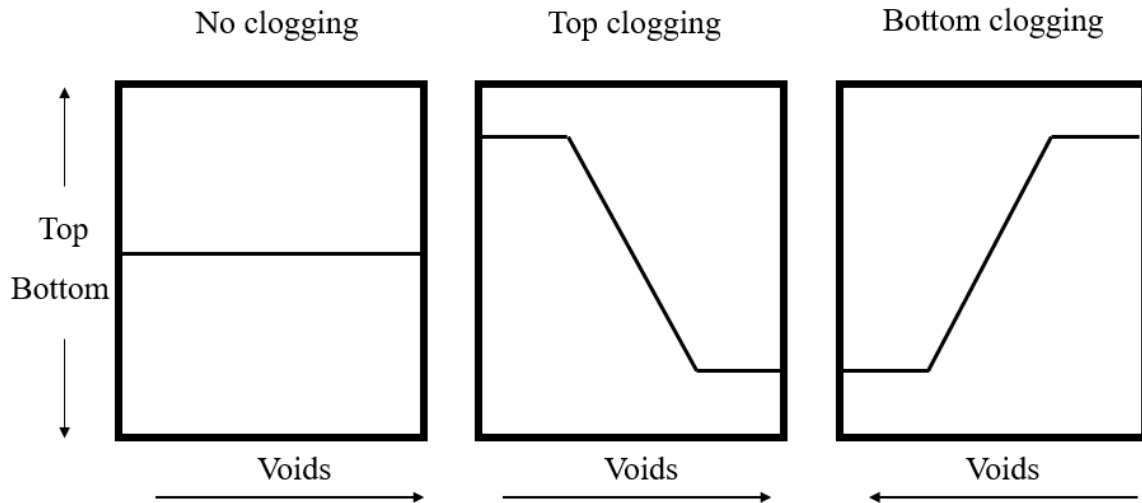
Figure 24 Three possible behaviours of the voids: 1) On the left, 2) In the middle and 3) On the right

The three behaviours from Figure 24 can easily be explained. When the measured constant of a pavement on a certain location at a certain moment in time increases this means there is less influence of air, since it has a dielectric constant of 1, (voids). So, the clogging increases. This linear reasoning is illustrated by Figure 25.

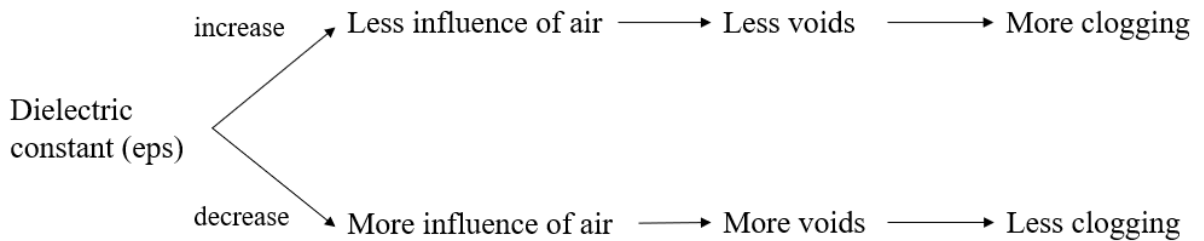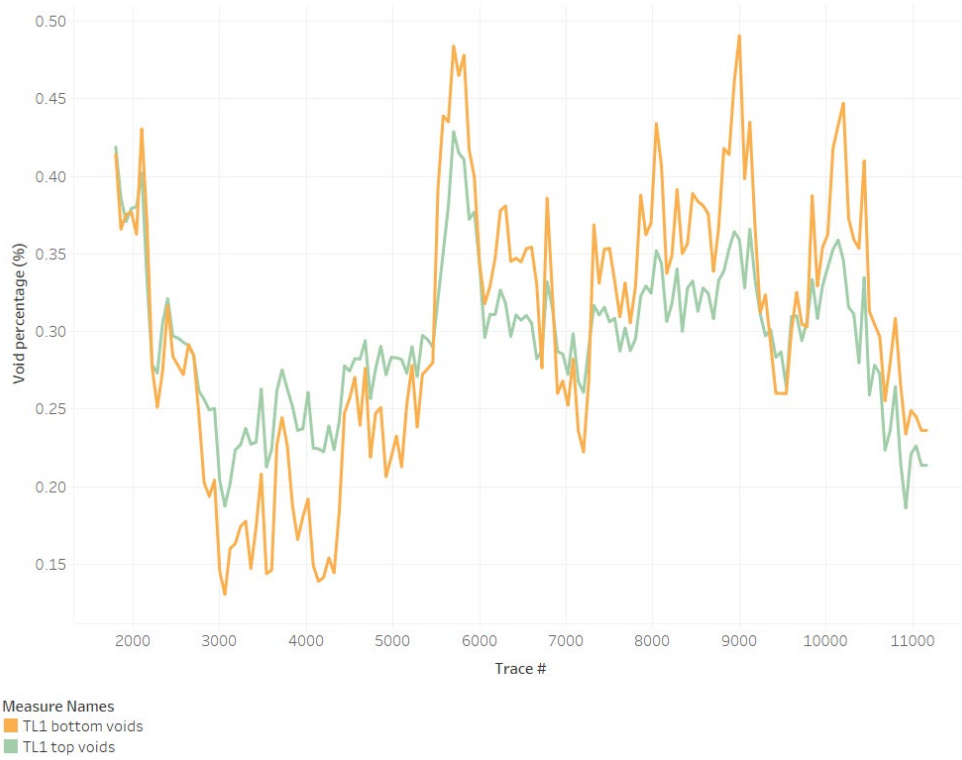*Figure 25 Reasoning how different DC's lead to difference in clogging.*

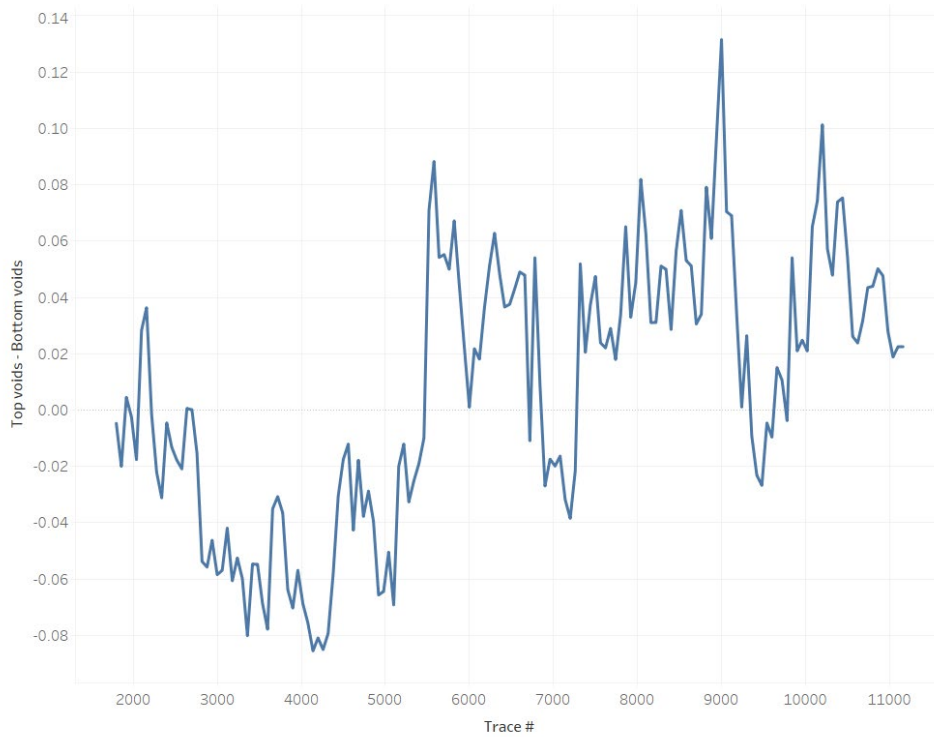*Figure 26 Smoothed void percentages along the segment at TL1*

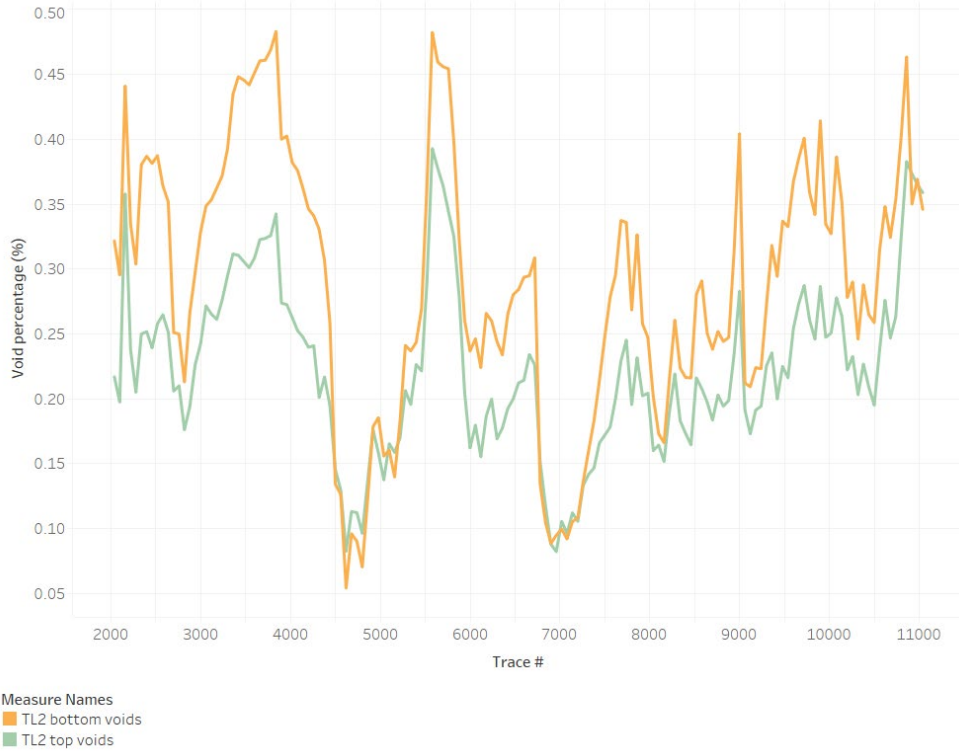*Figure 27 Void differences along the segment at TL1*

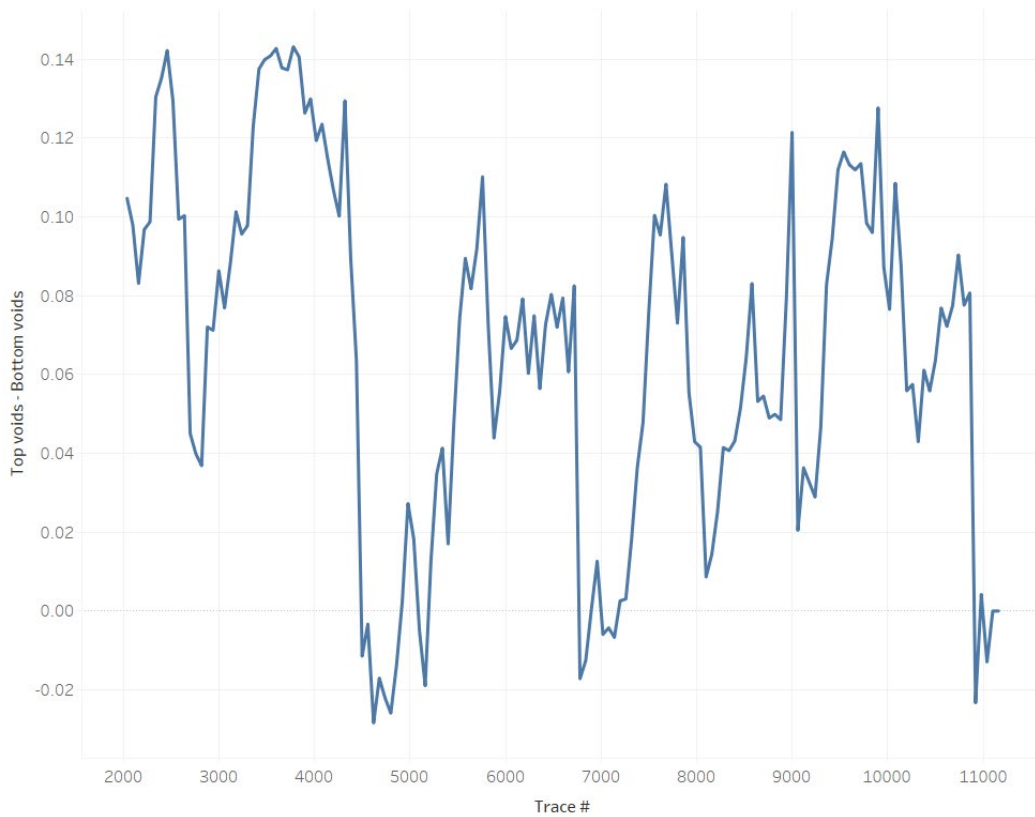*Figure 28 Smoothed void percentages along the segment at TL2*

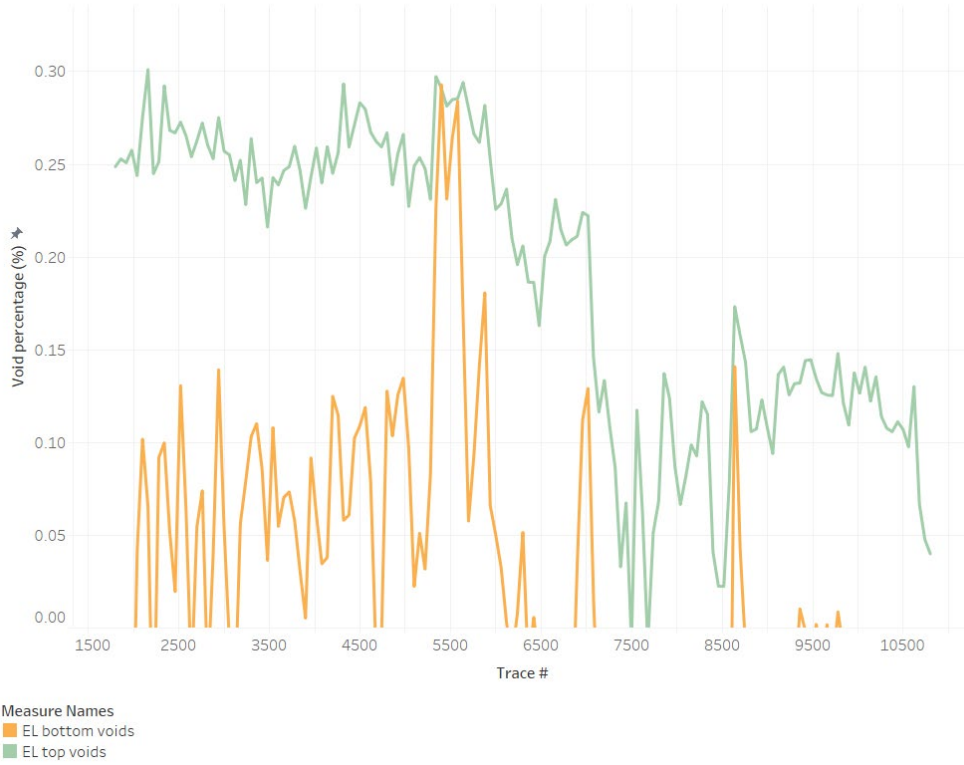*Figure 29 Void differences along the segment at TL2*

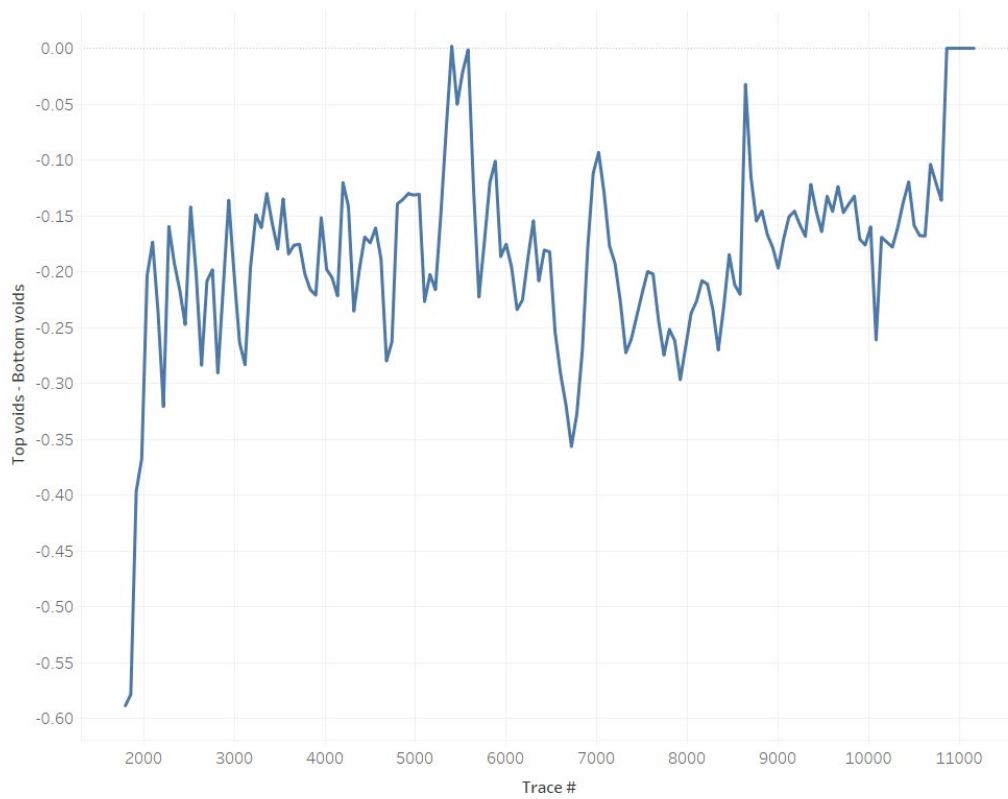*Figure 30 Smoothed void percentages along the segment at EL*

Figure 31 Void differences along the segment at EL

From all the observed descriptions of the data and measurements several things can be concluded. First of all the three lanes shows similar behaviour. On all three roads roughly three stages can be identified, see Figure 21. Between these three stages different behaviour of the measurements is visible. No clear conclusions can however be drawn to why these different stages are apparent. Also the void percentages and observed differences throughout the top layer seem reasonable looking at theoretical estimations from section 6.2.4 and literature.

Next to this also the three lanes clearly show high void peaks underneath the two overhanging structures. This could be explained since the pavement is harder to reach for clogging material from the air since it is protected by the overhanging structure.

In TL2 almost everywhere the voids increase, so behaviour 2 (middle in Figure 24) or top clogging is observed. This can probably be explained by cross-sectional movements by cars due to the entrance and exit around the segment and therefore clogging material in the top of the layer. This top clogging indicates a different material deposition than in bottom clogging and can be better explained by a different phenomenon namely smearing by car tires (Tiwari et al., 2021). This would mean that the heavy road use on TL2 results in this type of material deposition and therefore falls under a different type of porous pavement deterioration. This phenomenon is also observed in an older research performed by De Wegenscanners at a race circuit in 2004 (Limburg et al., 2004).

On the EL clear bottom clogging is observed, this is behaviour number 3 in the last section and shown in the right in Figure 24. This can be explained by clogging from the bottom as material deposition. This is the type of clogging this research strives to address. On average the EL shows a decrease in the amount of voids, so therefore clogging, of 18.5% on this particular segment under these conditions. The observed clogging clearly means the EL should be cleaned to prevent bottom clogging since it undermines the permeability it was intended to have.

On TL1 a middle ground is observed between TL2 and the EL. There are sections where bottom clogging is observed but also sections where top clogging is observed. This could be caused by a relatively more varying road use compared to TL2, where there is constant heavy use. Also the cross-sectional vehicle movements are predicted to be less than on TL2. So TL1 can partially be of interest when looking at clogging.

6. External validation roadmap

A major drawback or limitation of the internal validation that was described in the last chapter is that the method is performed on one case study of historic data. This means all the performed analyses are done on this specific road at this specific moment in time. It therefore lacks to give any estimation for the speed at which, for example the bottom clogging occurs in the emergency lane. Or it is near impossible to give an accurate indication for the state the A73 was in when it was measured last year, how clogged it already was at the time. In addition to this, the results from the measurements and the differences that were observed are under influence of numerous variables, like the asphalt mix used and the weather on the segment over its lifespan, that could affect the results greatly. All these factors restrain the significance of the results based on a set of historic data and therefore question the general applicability of the new measuring method. However, more research and more monitored data analyses could potentially enhance this significance and general applicability of the method. So in this chapter the roadmap will be described to further external validation of the new designed measuring method using GPR.

6.1. Periodic measurements

A first possible way to further externally validate the measuring method is by performing periodic measurements of a segment of road. Over time a growing dataset could offer increasingly more detailed insight in the speed at which a porous asphalt road clogs. Since a Dutch porous asphalt road (ZOAB) has a lifespan of about 11-15 years (Rijkswaterstaat, 2020) biannual measurements can secure a healthy growing dataset and at the same time enable application of reliable results on the same road for more efficient road management. Another advantage of this method is that it keeps improving itself if the dataset keeps growing. Monitoring conditions of roads and connecting those to the clogging estimations will also establish better predictions for future comparable roads.

A drawback of this method is that it is time consuming. Perseverance in regular measurements is key to assure reliable conclusions but time needed and therefore clients to get the healthy dataset required might be a limitation for De Wegenscanners. Another limitation might be

the complexity of the dataset. When it keeps growing and more conditions are monitored the complexity of it all might outgrow the possibilities for De Wegenscanners. This can be counteracted by carefully assessing which conditions are of great influence and which are not and in doing so further refine the GPR method.

So periodic measurements could function as an external validation method but the practical implementation might only be partially interesting for De Wegenscanners. The more measurements of monitored segments they do the better but finding projects to measure a porous road for years can be the challenge.

6.2. Comparison with Becker test

Another way to externally validate the method is by comparing it with the well-known Becker test, described in section 3.1. The Becker test is the way permeability of porous asphalt is currently measured. The amount of voids, which the GPR method determines, is closely related to the permeability of the pavement. Some assumptions need to be made however to gap the bridge between the void percentage of a pavement and its permeability, like interconnectivity of the voids and other topological characteristics such as its tortuosity. On the other hand the widely applied Becker test might already indicate void percentages next to permeability bridging the gap towards GPR. Nevertheless, comparisons with Becker tests can extend the field for GPR applications and by doing that validate the method described in this research along the way. De Wegenscanners are currently performing a validating project where also Becker tests are added to compare to the GPR method from this research. The results will show to which extent this comparison validates the GPR method or that it suits as an addition to other external validation methods.

6.3. Measurements before and after cleaning

A third method to validate the GPR method can be by taking measurements of a pavement segment before and after cleaning. ZOAB roads are currently periodically cleaned by a high pressure vacuum cleaner. A comparison between measurements just before and right after can validate the method, especially in combination with another comparison like the Becker test described above. This method of validating is relatively time efficient, since only two measurements need to be

performed. Furthermore, it could also offer insight in the effectiveness of pavement cleaning, something that is more often questioned than understood.

For this method and probably all methods it must be said that based on the internal validation done in this research the preference should be on the emergency lane since it showed significant bottom clogging, see section 6.2.6. Next to this, the emergency lane is the lane of most interest since that is the lane which is desired to be the most permeable. If a project on an emergency lane is not available a left lane is the next to show some prospects, based on the performed internal validation. De Wegenscanners are currently performing a validating project like this where a left lane is measure before and after cleaning, drill core tests are performed as well as Becker tests. The results of this project could be the next step towards GPR application for clogging measurements.

6.4. Experimental setup

Finally, an experimental setup could function as an external validation method. In such a setup boundary conditions which are numerously mentioned in this research like mix design and weather conditions can be controlled to improve the compatibility of different GPR measurements. Next to that, it could be time efficient if for example clogging cycles represent several years of use. Also variables can be adjusted to test out different behaviours such as the difference between smearing and clogging which were both observed in the internal validation.

The limitation of the described validating method is that it remains a simulated setup. This could limit the applicability of the GPR method in practice. It could be counteracted by attempting to simulate real porous pavements scenario's but that might be a quite challenging.

However, for De Wegenscanners experiments could be of great interest in the beginning of validating the method. They would not rely on time consuming projects but could simulate at their own pace and with it expand their expertise and general research into the GPR method for clogging.

The above mentioned external validation methods show possible prospects for further establishment of the GPR measuring method. While all of them have their own limitations a combination of the methods promises to be the most fruitful. This is exactly what De Wegenscanners are planning to do in the future since the internal validation on the case study in this research proves the working of the GPR measuring method sufficiently and with it extend their expertise in the field of GPR measurements to improve road management.

7.   Conclusions

For this research several conclusions can be drawn. The main conclusion is to what extent the research answers the formulated research question. This main research question is defined in section 3.3 as "*How and to which extent can the GPR data evaluation method quantify clogging in Dutch porous asphalt pavement roads (ZOAB) to enable predictive maintenance?*".

The first part of the question entails something about the design of the new GPR measuring method since it asks how GPR data evaluation can quantify clogging. The answer to this is described in section 5.1 where all preparation and processing steps are extensively outlined. In short, de top layer of the pavement is highlighted in the radargram after which the measured reflection amplitudes are exported for each data point some decimetres apart. Then mathematical formulas are applied to the data to determine dielectric constants for all the locations. These dielectric constants are transformed into void percentages and the difference between the void percentage on top and on the bottom of the porous asphalt layer are visually analysed. During this final analysis several conditions like the type of asphalt used and the weather conditions during the measurements need to be taken into account, more on this in section 6.1. So, the first part of research question is extensively answered in the design of the new method and during the validating case study.

The second part of the research question asks to what extent the results from the GPR data evaluation method can truly predict clogging in porous pavements. The answer to this question is partly answered by the internal validation in the case study. Next to this, Chapter 7 describes external evaluation methods that could serve as method to further answer this part of the research question. Based on the validating case study the GPR measuring method identifies clogging clearly on the emergency lane (EL). The emergency lane for the analysed segment showed an average 18.5% decrease in the amount of voids. This decrease underlines the need for more clogging measurements and cleaning on the emergency lanes. Rather than this quantitative percentage the qualitative void behaviour observed indicates that GPR offers prospects to function as clogging estimation method but more research is needed to examine the right relationship between voids and the dielectric constant and the averaging of the data points. But the qualitative void behaviour observed shows

possibilities for GPR to improve efficient road management. For the right traffic lane (TL2) top clogging is observed, which is not the intended type of clogging for this research and it could better be explained by a phenomenon called smearing of asphalt pavements. The left traffic lane (TL1) shows a combination of bottom clogging and top clogging and therefore offers partial potential for application of the GPR method. It must be said that for the moment all lanes are still of interest for further application also to strengthen the conclusion of different types of clogging.

Next to this, the external validation methods illustrate what future researches should contain to establish the GPR data evaluation method further. The separate methods described have their limitations like still being time consuming or increasing the complexity of the data evaluation. However, they all show their potential for further establishment and perhaps a combination of several validating methods has the most potential. De Wegenscanners are currently performing a validating project of a left traffic lane and combine measurements before and after cleaning with a comparison with Becker tests. The results from this should prove the GPR method further and also examine if the validating methods function accordingly.

Overall, this research contributed to the introduction of GPR as measuring method for clogging in porous pavements. It designed a method how GPR data evaluation can be used for clogging estimations. The method was partially and qualitatively proven to work in an internal validating case study and the future developments of the GPR measuring method are prescribed. With it the research contributes to both De Wegenscanners for their future GPR explorations and for science as a new field for many researches to come.

8.   References

Abu Dabous, S., Yaghi, S., Alkass, S., & Moselhi, O. (2017). Concrete bridge deck condition assessment using IR Thermography and Ground Penetrating Radar technologies. *Automation in Construction*, *81*(April), 340–354. https://doi.org/10.1016/j.autcon.2017.04.006

Al-Qadi, I. L., & Lahouar, S. (2005). Measuring layer thicknesses with GPR - Theory to practice. *Construction and Building Materials*, *19*(10), 763–772. https://doi.org/10.1016/j.conbuildmat.2005.06.005

Beheerraad Aanbesteden en Contracteren, & CROW. (2020). *Herziening Hoofdstuk 81 ' Bitumineuze verhardingen ' en enkele bijbehorende Proeven.*

Benedetto, A., Tosti, F., Bianchini Ciampoli, L., & D'Amico, F. (2017). An overview of ground-penetrating radar signal processing techniques for road inspections. *Signal Processing*, *132*, 201–209. https://doi.org/10.1016/j.sigpro.2016.05.016

Brovelli, A., & Cassiani, G. (2008). Effective permittivity of porous media : a critical analysis of the complex refractive index model. *Geophysical Prospecting*, *56*, 715–727. https://doi.org/10.1111/j.1365-2478.2008.00724.x

Burningham, S., & Stankevich, N. (2005). *Why road maintenance is important and how to get it done*. 94–102. https://doi.org/10.4324/9781351175746-8

Ciampoli, L. B., Tosti, F., Economou, N., & Benedetto, F. (2019). Signal processing of GPR data for road surveys. *Geosciences (Switzerland)*, *9*(2). https://doi.org/10.3390/geosciences9020096

Cosenza, P., Marmet, E., Rejiba, F., Jun Cui, Y., Tabbagh, A., & Charlery, Y. (2006). Correlations between geotechnical and electrical data: A case study at Garchy in France. *Journal of Applied Geophysics*, *60*(3–4), 165–178. https://doi.org/10.1016/j.jappgeo.2006.02.003

De Wegenscanners. (2020). *Wat doen we*. https://dewegenscanners.nl/wat-doen-we/

Dube, D. C. (1970). *Study of Landau-Lifshitz-Looyenga ' s formula for dielectric correlation between powder and bulk. 1648.*

ECMT, & OECD. (2002). Implementing sustainable urban travel policies. In *Public Transport International* (Vol. 51, Issue 1). https://doi.org/10.1787/9789282113172-en

Fauchard, C., Li, B., Laguerre, L., Héritier, B., Benjelloun, N., & Kadi, M. (2013). *Determination of the compaction of hot mix asphalt using high-frequency electromagnetic methods. 60*, 40–51. https://doi.org/10.1016/j.ndteint.2013.07.004

Fuller, C. J. F. B., & Jr., W. F. B. (1953). *Theory of Electric Polarisation. 17.* https://doi.org/10.1063/1.3061227

Fwa, T. F., Tan, S. A., & Guwe, Y. K. (1999). Laboratory evaluation of clogging potential of porous asphalt mixtures. *Transportation Research Record*, *1681*, 43–49. https://doi.org/10.3141/1681-06

Garcia, A., Aboufoul, M., Asamoah, F., & Jing, D. (2019). Study the influence of the air void topology on porous asphalt clogging. *Construction and Building Materials*, *227*, 116791. https://doi.org/10.1016/j.conbuildmat.2019.116791

GSSI Academy. (2020). *GSSI Academy: Understanding the Dielectric Constant.* https://www.geophysical.com/gssi-academy-understanding-the-dielectric-constant#:~:text=GPR Theory%3A Understanding the Dielectric,%2C gravel%2C or other material.&text=This constant describes the speed,move through a particular material.

Hamzah, M. O., Abdullah, N. H., Voskuilen, J. L. M., & van Bochove, G. (2013). Laboratory simulation of the clogging behaviour of single-layer and two-layer porous asphalt. *Road Materials and Pavement Design*, *14*(1), 107–125. https://doi.org/10.1080/14680629.2012.749803

Hoegh, K., Khazanovich, L., Dai, S., & Yu, T. (2015). Case Studies in Nondestructive Testing and Evaluation Evaluating asphalt concrete air void variation via GPR antenna array data. *Case Studies in Nondestructive Testing and Evaluation*, *3*, 27–33. https://doi.org/10.1016/j.csndt.2015.03.002

Jouyban, A., Soltanpour, S., & Chan, H. (2006). A simple relationship between dielectric constant of mixed solvents with solvent composition and temperature. *International Journal of Pharmaceutics*, *269*(2004), 353–360. https://doi.org/10.1016/j.ijpharm.2003.09.010

KNMI. (2020). *Neerslag 29 KNMI weerstations*. weerdata.nl/index.php?meting=neerslag

Leegwater, G., Lent, D. van, Roetert Steenbruggen, K., Luiten, B., Groenendijk, J., & Schipper, M. (2019). *Inventarisatie levensduurvoorspellende modellen voor asfalt.*

Leng, Z. (2011). *PREDICTION OF IN-SITU ASPHALT MIXTURE DENSITY USING GROUND PENETRATING RADAR : THEORETICAL DEVELOPMENT AND FIELD VERIFICATION.*

Leng, Z., Al-qadi, I. L., & Lahouar, S. (2011). NDT & E International Development and validation for in situ asphalt mixture density prediction models. *NDT and E International*, *44*(4), 369–375. https://doi.org/10.1016/j.ndteint.2011.03.002

Limburg, H., Koomans, R., & Groenboom, R. (2004). *Change in circuit roughness Braga , PT TrackMAP feasibility test Confidential. September.*

Ma, X., Jiang, J., Zhao, Y., & Wang, H. (2020). Characterization of the interconnected pore and its relationship to the directional permeability of porous asphalt mixture. *Construction and Building Materials*, *xxxx*, 121233. https://doi.org/10.1016/j.conbuildmat.2020.121233

Ma, Y., Chen, X., Geng, Y., & Zhang, X. (2020). Effect of Clogging on the Permeability of Porous Asphalt Pavement. *Advances in Materials Science and Engineering*, *2020*. https://doi.org/10.1155/2020/4851291

Madhu Lisha Pattanaik, Rajan Choudhary, B. K. (2017). *Clogging evaluation of open graded friction course mixes with EAF steel slag and modified binders* (p. 14). Construction and Building Materials.

Maślakowski, M., Kowalczyk, S., Mieszkowski, R., & Józefiak, K. (2014). Using electrical resistivity tomography (ERT) as a tool in geotechnical investigation of the substrate of a highway. *Studia Quaternaria*, *31*(2), 83–89. https://doi.org/10.2478/squa-2014-0008

Moriyoshi, A., Jin, T., Nakai, T., & Ishikawa, H. (2013). Evaluation methods for porous asphalt pavement in service for fourteen years. In *Construction and Building Materials* (Vol. 42, pp. 190–195). https://doi.org/10.1016/j.conbuildmat.2012.12.070

NAPA, & EAPA. (2011). *The Asphalt Paving Industry. 2*, 36. http://www.asphaltpavement.org/images/stories/GL_101_Edition_3.pdf

Nelson, S. O. (2005). *Density-Permittivity Relationships for Powdered and Granular Materials. 54*(No. 5 November 2005). https://doi.org/10.1109/TIM.2005.853346

OECD. (2002). Road Travel Demand. In *Road Travel Demand*. https://doi.org/10.1787/9789264175518-en

Opzoekingscentrum voor de Wegenbouw. (2018). *Ontwikkeling van de grondradartechniek voor wegconditieonderzoek.* 136.

PAVEMENT STRUCTURE EVALUATION USING GPR. (n.d.). Retrieved March 12, 2021, from https://gprpavement.com/

Pellinen, T., Eskelinen, P., Huuskonen-Snicker, E., & Hartikainen, A. (2015). *Assessment of air void content of asphalt using dielectric constant measurements by GPR and with VNA*. School of Engineering.

PLM. (2019). *WHAT ARE THE DIFFERENT TYPES OF ASPHALT?* https://www.plmpaving.com/articles/what-are-the-different-types-of-asphalt

Rijkswaterstaat. (2005). *Toename ZOAB-areaal op basis van de deklaagplanning* (p. 1).

Rijkswaterstaat. (2020). *Zoab*. Aanleg Wegen.

Ruppin, R. (2000). *Evaluation of extended Maxwell-Garnett theories. August*, 273–279.

Saarenketo, T. (2006). *Electrical properties of road materials and subgrade soils and the use of Ground Penetrating Radar in traffic infrastructure surveys*.

Saarenketo, T., & Scullion, T. (2000). Road evaluation with ground penetrating radar. *Journal of Applied Geophysics*.

Sansalone, J., Asce, M., Kuang, X., & Ranieri, V. (2008). *Permeable Pavement as a Hydraulic and Filtration Interface for Urban Drainage. October*, 666–674.

Schaefer, V. R., & Kevern, J. T. (2011). *An Integrated Study of Pervious Concrete Mixture Design for Wearing Course Applications An Integrated Study of Pervious Concrete Mixture Design for Wearing*.

Scholz, M., & Grabowiecki, P. (2007). Review of permeable pavement systems. *Building and Environment*, *42*(11), 3830–3836. https://doi.org/10.1016/j.buildenv.2006.11.016

Shutko, A. M., & Reutov, E. M. (1982). Mixture Formulas Applied in Estimation of Dielectric and Radiative Characteristics of Soils and Grounds at Microwave Frequencies. *IEEE Transactions on Geoscience and Remote Sensing*, *1*, 29–32.

Solla, M., Lagüela, S., González-Jorge, H., & Arias, P. (2014). Approach to identify cracking in asphalt pavement using GPR and infrared thermographic methods: Preliminary findings. *NDT and E International*, *62*, 55–65. https://doi.org/10.1016/j.ndteint.2013.11.006

Swanson, L. (2001). Linking maintenance strategies to performance. *International Journal of Production Economics*, *70*(3), 237–244. https://doi.org/10.1016/S0925-5273(00)00067-0

Tiwari, A., Miyashita, N., & Persson, B. N. J. (2021). Rubber Wear and the Role of Transfer Films on Rubber Friction on Hard. *Tribology Letters*, *69*(2), 1–12. https://doi.org/10.1007/s11249-021-01410-4

Tong, B. (2011). *Clogging effects of portland cement pervious concrete*.

VBW. (2016). *Richtlijn Tweelaags ZOAB*. 1–26.

Wyseure, G. (2006). *Simultaan meten van bodemwater-gehalte en electrische conductivi-teit (EC) door middel van TDR.pdf*. Katholieke Universiteit Leuven, Geo-instituut Afdeling Bodem en Waterbeheer.

Yadav, A. S., & Parshad, R. (1971). On the utilization of Böttcher's formula for correct correlation of dielectric constant of powder and bulk On the utilization of Bottcher's formula for correct correlation of dielectric constant of powder and bulk. *Journal of Physics D: Applied Physics*, *4*, 6–9.

Yong, C., Deletic, A., Fletcher, T. D., & Grace, M. R. (2008). The clogging behaviour and treatment efficiency of a range of porous pavements. *11th Int. Conference on Urban Drainage, March 2014*, 1–12. http://www.permapave.com.au/technical/downloads/Permapave_Clogging_report_(USletter).pdf

Zhao, Y., Wang, X., Jiang, J., & Zhou, L. (2019). *Characterization of interconnectivity, size distribution and uniformity of air voids in porous asphalt concrete using X-ray CT scanning images* (p. 12). Construction and Building Materials.